

# Molecular gas in distant galaxies from ALMA studies

Françoise Combes

Received: date / Accepted: date

**Abstract** ALMA is now fully operational, and has been observing in early science mode since 2011. The millimetric (mm) and sub-mm domain is ideal to tackle galaxies at high redshift, since the emission peak of the dust at  $100\mu\text{m}$  is shifted in the ALMA bands (0.3mm to 1mm) for  $z=2$  to 9, and the CO lines, stronger at the high-J levels of the ladder, are found all over the 0.3-3mm range. Pointed surveys and blind deep fields have been observed, and the wealth of data collected reveal a drop at high redshifts ( $z > 6$ ) of dusty massive objects, although surprisingly active and gas-rich objects have been unveiled through gravitational lensing. The window of the reionization epoch is now wide open, and ALMA has detected galaxies at  $z=8-9$  mainly in continuum, [CII] and [OIII] lines. Galaxies have a gas fraction increasing steeply with redshift, as  $(1+z)^2$ , while their star formation efficiency increases also but more slightly, as  $(1+z)^{0.6}$  to  $(1+z)^1$ . Individual object studies have revealed luminous quasars, with black hole masses much higher than expected, clumpy galaxies with resolved star formation rate compatible with the Kennicutt-Schmidt relation, extended cold and dense gas in a circumgalactic medium, corresponding to Lyman- $\alpha$  blobs, and proto-clusters, traced by their brightest central galaxies.

**Keywords** Galaxies · Early Universe · Re-ionization · molecules

## 1 Introduction

The recent years have seen a breakthrough in the domain of high redshift galaxies, and in particular in the knowledge of their molecular gas and their

---

F. Combes  
Observatoire de Paris, LERMA, Collège de France, CNRS, PSL Univ., Sorbonne University,  
UPMC, Paris, France  
Tel.: +33-1-40512077  
Fax: +33-1-40512002  
E-mail: francoise.combes@obspm.fr

star formation with ALMA. While the uv/optical/infrared domains give information on the star formation density, and its evolution in the Universe (e.g. Madau and Dickinson, 2014), the efficiency of star formation requires knowledge of the gas content. Molecular gas is the fuel of star formation, and its observation is necessary to understand galaxy formation.

ALMA with its 66 dishes (54 antennae of 12m and 12 antennae of 7m, located in a unique high and dry site, has increased the power of previous (before 2010) millimetric arrays by an order of magnitude. Baselines from 20m to 16km, at wavelengths between 3mm to 0.3mm, provide spatial resolutions up to 15mas. The large bandwidth of 7.5 GHz/polar ensures a high sensitivity for continuum observations, and allows to search and determine redshifts. ALMA is well adapted for deep fields, but not for big surveys, the field of view is from 1 arcmin (at 3mm) to 6 arcsec (at 0.3mm). Mapping small regions with mosaics is very efficient.

The main advantage for high redshift galaxies is that the peak of dust emission usually around 100 microns, for star forming objects, is redshifted to the submm and mm domain. This produces a negative K-correction, i.e. continuum emission from dust is as easy to detect at  $z=10$  than at  $z=1$  (e.g. Blain et al, 2002). Already in the pre-ALMA era, it was possible to detect hundreds of high- $z$  galaxies with  $L(\text{IR}) > 10^{12} L_{\odot}$ , up to  $z=6$  (e.g. Omont, 2007). The large derived dust masses of  $\sim 10^8 M_{\odot}$ , mean that dust forms early in the universe. These sub-millimeter galaxies (SMG) contribute significantly to the sub millimetre background, their redshift distribution peaks at  $z=2-3$  (Chapman et al, 2005).

For the CO lines, there is no negative K-correction, although the flux is higher at the upper levels of the ladder (high J), when the gas is dense enough (e.g. Combes et al, 1999). Distant galaxies have started to be explored in molecular lines in 1992, with lensed objects (Brown and Vanden Bout, 1992; Downes et al, 1995), and line detections followed at a high rate, about 50 objects up to  $z=6.4$  with the quasar J1148+5251 (Cox, 2005; Maiolino et al, 2005).

With ALMA, it is now possible to detect CO lines in a large amount of high- $z$  galaxies, even not amplified by gravitational lensing. It is possible to discover obscured objects in deep fields, from their dust emission, and search for their redshift, when it is not possible in the optical domain. For  $z>6$  galaxies, the high-J CO lines ( $J>7$ ) are observed at low frequencies (3mm) with a field of view of 1 arcmin, and a bandwidth of  $2 \times 8\text{GHz} \sim 16\%$ , or 50 000km/s. At  $z=6$ , the spacing between the various CO lines of the rotational ladder is of 16 GHz, so that the redshift may be obtained with 2 tunings only.

This review highlights the main results of ALMA observations of distant galaxies, from the dust emission to molecular lines. The CO are the most usual gas tracers, but at very high  $z$ , the [CII] and CI lines bring important information, in a domain where the CO lines are not or little excited. Dense gas tracers (HCN,  $\text{HCO}^+$ , CS, etc) and isotopes, bring complementary knowledge on gas properties, and are frequently observed simultaneously, thanks to the wide bandwidth of ALMA.

The review emphasizes only the recent results since the previous reviews in the domain, pre- or post-starting of ALMA Solomon and Vanden Bout (2005); Carilli and Walter (2013).

## 2 The CO lines as tracer of the molecular gas

The main  $H_2$  molecule is symmetric and has no dipolar transition. At the low temperature of the interstellar medium ( $\sim 20K$ ), the quadrupolar transitions are not excited, and moreover they have a very weak Einstein coefficient. The main tracer of the molecular gas is then the CO molecule (with solar abundance of  $CO/H_2 \sim 10^{-4}$ ), tracing the bulk of the gas, with a critical density of the order of  $10^3$ - $10^4 \text{ cm}^{-3}$  for the lowest levels. Other molecules with a higher critical density (more than 2 orders of magnitude higher), like HCN,  $HCO^+$  or CS are used as high density tracers. Their intensity is usually 10-30 times lower.

### 2.1 Emission lines

At high redshift, the large advantage of the CO tracer is the high probability to find any line J from the rotational ladder, since the ladder spacing decreases as  $(1+z)^{-1}$ ; and when the gas is excited, the line strength of the J levels increases almost as the square of the frequency. There are good reasons to expect higher density molecular gas in high- $z$  galaxies (they are more gas rich, and their volumic density is higher), such that higher excitation is the norm. This situation favors the detection of molecular gas at high- $z$ , while the atomic gas has large difficulties with the unique 21cm line.

The distribution of radiating energy among the various J-lines of the CO ladder called the SLED (Spectral Line Energy Distribution), is a very useful diagnostic of the physics of the emitting interstellar medium (ISM), in particular its density and temperature. It has been shown that the CO SLED can distinguish between quiescent Milky Way-like galaxies, where the emission is peaking at  $J=3$ , and dense and warm starbursts, where the peak is up to  $J=8$  (Weiß et al, 2007). These excitations come from star formation processes (PDR, or photo-dissociation regions), but near AGN, higher excitation is possible, in particular through hard X-rays (XDR, or X-ray dominated regions) (van der Werf et al, 2010). In some cases of very concentrated starbursts, the dust opacity could also perturb the SLED (Papadopoulos et al, 2010).

At high redshift, galaxies have a higher gas fraction, the gas is denser, and star formation rates are higher in average. It is therefore expected that the CO lines are more excited, favoring the detection of the molecular gas. There is also the possibility of radiative excitation from the cosmic background, which temperature varies in  $(1+z)$ , reaching  $\sim 30K$  at  $z=9$ . It is not obvious that this excitation helps the detection, since the detected signal is only the excess above

the background. This has been simulated, and indeed, there is no negative K-correction for the CO lines, contrary to the dust continuum emission, (e.g. Combes et al, 1999; da Cunha et al, 2013).

The derivation of the molecular content from the CO lines relies on the CO-to-H<sub>2</sub> conversion factor, well calibrated at low redshift, and in particular in the Milky Way: clouds are then detected individually, and their virial masses estimated. The conversion factor has a robust statistical value, when averaged over a large cloud population, with a wide range of masses and densities. The factor depends however strongly on gas metallicity (e.g. Bolatto et al, 2013). It is possible to quantify the fraction of diffuse and clumpy components, with high density tracers such as HCO<sup>+</sup>, HCN, allowing to refine the conversion factor. For example Oteo et al (2017) have shown with ALMA that the excitation of HCO<sup>+</sup>, HCN and HNC in two lensed dusty starbursts at  $z \sim 2$  is very similar to what is already known in local IR-bright galaxies. Due to the virial hypothesis, the conversion factor is thought to vary as the square root of the H<sub>2</sub> volumic density, divided by the brightness temperature of the clouds,  $\propto n(\text{H}_2)^{1/2}/T_B$ . In local starbursts, both the cloud brightness and their density increases, which limits the variation of the ratio (e.g. Leroy et al, 2011). The metallicity is however a serious problem, since it is thought to decrease with redshift. Using one of the first large surveys of star forming galaxies at  $z > 1$ , Genzel et al (2012) have estimated the variation of the conversion factor with metallicity (see Figure 1).

## 2.2 Absorption lines

A complementary way to probe the interstellar medium of high redshift galaxies is from absorption lines in front of a strong millimeter continuum source. These molecular lines can provide information on the chemistry and its evolution with  $z$ , and also the physical conditions of the gas (density, temperature). The lines may be very narrow ( $< 1\text{km/s}$ ) and useful to constrain the variations of fundamental constants. The absorbing systems before ALMA were only 4-5 (e.g. Combes, 2008). With ALMA, it was possible to carry on a molecular survey towards the system PKS1830-211, corresponding to two gravitational images and an Einstein ring in the absorbing foreground lens (Muller et al, 2014). In particular, isotopes of the chloronium were detected, and OH<sup>+</sup>, H<sub>2</sub>O<sup>+</sup> have allowed to measure the molecular gas fraction and the ionization rate of the gas, in several lines of sight (Muller et al, 2016). With ALMA, new molecular lines are detected in  $z=0.5-1$  absorbers (e.g. Wiklind et al, 2018), but also a large number in more local radio sources (David et al, 2014; Tremblay et al, 2016), where the absorptions are determinant to disentangle inflows from outflows.

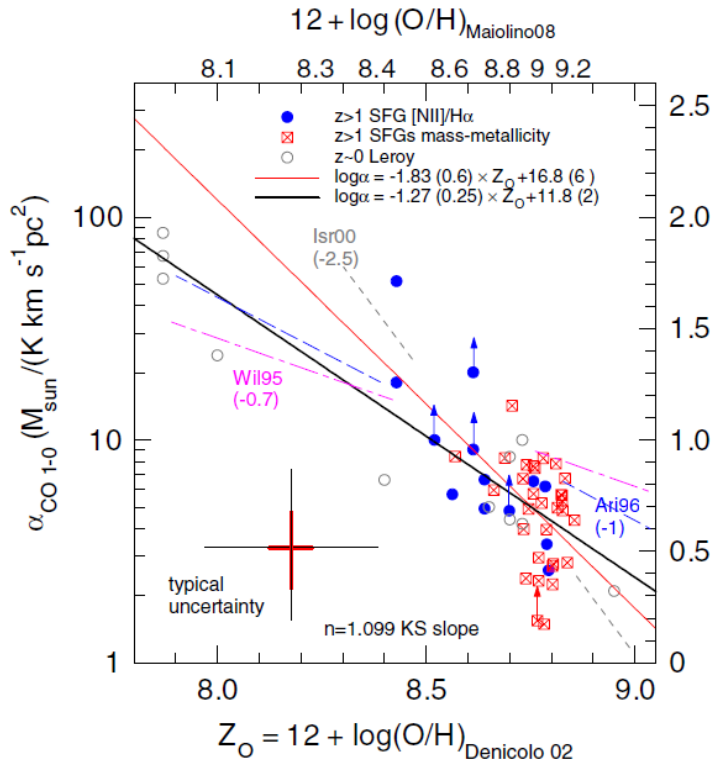


**Fig. 1** The derived conversion factor between the CO(1-0) luminosity and the molecular gas mass,  $\alpha_{CO}$  as a function of metallicity in the gas phase. The molecular gas mass is computed independently of the CO luminosity from the SFR and the Kennicutt-Schmidt (KS) relation, with a slope  $n=1.1$ . The gray circles are for local galaxies (Leroy et al, 2011). The gas metallicity for high-z blue-symbol galaxies have been obtained from the [NII]/H $\alpha$  flux ratio, converted to oxygen abundance scale from Denicoló et al (2002) and Maiolino et al (2008). The red symbols are galaxies where metallicity is derived from the total stellar mass. Image reproduced with permission from Genzel et al (2012), copyright by AAS.

### 3 Dust emission as a molecular gas tracer

Although the CO molecule is arguably the best tracer of the H<sub>2</sub> content of a galaxy, it is primordial to gather results from several tracers, to inter-compare them, and avoid some of the main biases of any given diagnostic. At high redshift, this is even more required, since the CO lines observed are from a high J-level, and several CO lines are needed to derive the gas excitation, and estimate the CO(1-0) intensity calibrated in terms of H<sub>2</sub> mass. The main alternate tracer is the dust continuum emission in the Rayleigh Jeans domain (i.e. close to the CO(4-3) to CO(7-6) if excited), where the dust emission is linear in both temperature and column density. The assumed dust-to-gas ratio will account for metallicity effect. Other tracers at very high z are fine structure

line emission such as the [CII] at  $158\mu\text{m}$ , or the [OIII] at  $88\mu\text{m}$ , with some specificity as gas tracers, as will be developed in Section 6.

Casey et al (2014) have written a detailed review of far-infrared and sub-millimeter survey of high redshift galaxies with dust emission. Although the temperature of the dust heated by star formation in molecular clouds, is expected in average of the order of 20-40K, in some cases, nuclear starbursts or AGN, the dust can peak at 60K. This produces large uncertainties in the detection rates of continuum surveys, since their success rate depends in the SED distribution of the sources.

Scoville et al (2014, 2016) have proposed that the Rayleigh-Jeans tail of the dust emission spectrum, peaking around  $100\mu\text{m}$ , acts as a good tracer of the gas content of galaxies: the Rayleigh-Jeans regime means that the dust temperature is involved only linearly, and does not introduce too much uncertainty. Of course the dust abundance is also proportional to metallicity, so the conversion factor between the dust emission and gas mass, through the dust-to-gas ratio, is as uncertain as the CO method. However, the detection of the dust continuum might be easier than the line, and does not require specific tunings. In compensation, there is more confusion and no redshift or kinematical information on the detected objects. While it is relatively easy to detect actively star forming galaxies and starbursts, main sequence objects at relatively low redshifts are more difficult to detect in dust continuum than in the CO lines, given the non-linear  $L_{FIR}$ - $L_{CO}$  scaling relation. For instance, in a sample of normal star-forming galaxies of the COSMOS field at  $z \sim 3$ , about half of the galaxies are detected in continuum with ALMA, and the rest of the undetected sources have to be stacked (Schinnerer et al, 2016). Besides, the CO line observation provides more very useful information as the dynamical mass, and gas excitation.

Another difference between dust and CO tracers, is that the former traces both atomic and molecular gas. A calibration experiment has shown however that at low and high redshift the two main tracers of the molecular/interstellar gas agree very well, see Figure 2.

#### 4 Galaxy surveys at high redshift

Although ALMA is not a large survey facility, it is of primordial importance to gather the properties (gas content and excitation, star formation rate, etc.) of a large number of objects, to gain a statistical significance, and to be able to split the samples in several categories, to explore the influence of parameters. Essential in the value of surveys are the selection criteria, for them to be representative even if flux-limited. Surveys have been done with carefully chosen criteria from multi-wavelength studies: these are pointed surveys when sources are already well-known (position,  $z$ , stellar mass, SFR). Another type of surveys is the deep field method, unbiased, but sometimes less successful, according to the choice of sensitivity required (shallow, deep), and the choice of tuning (continuum, lines, etc.). Blind surveys have however the immense

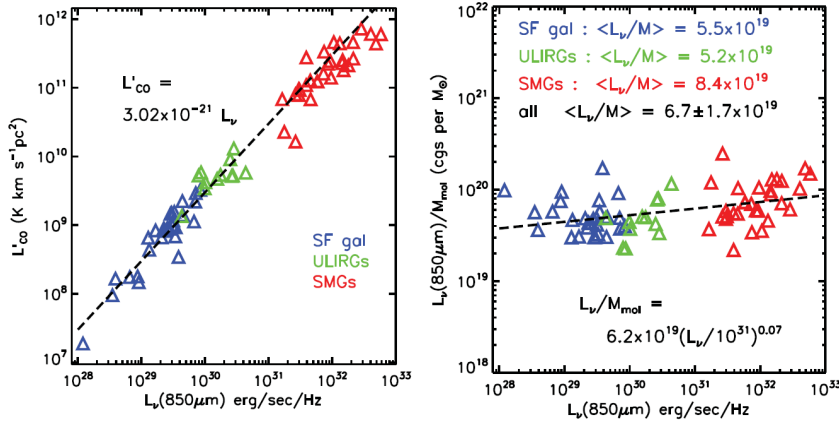


**Fig. 2** Comparison between the dust continuum and CO line tracers of the interstellar gas. The left panel compares the 850 $\mu\text{m}$  and CO luminosities for normal low- $z$  star forming galaxies (SF gal), low- $z$  ULIRGs, and  $z \sim 2$  submillimeter galaxies (SMG, many of them are lensed). At right, the ratio between these two luminosities ( $L'_{CO}$  being converted to  $M_{mol}$ ) shows in more detail an almost constant proportionality factor. The conversion factor used is  $M_{mol} = 6.5 L'_{CO}$  [K km/s pc $^2$ ]. Image reproduced with permission from Scoville et al (2016), copyright by AAS.

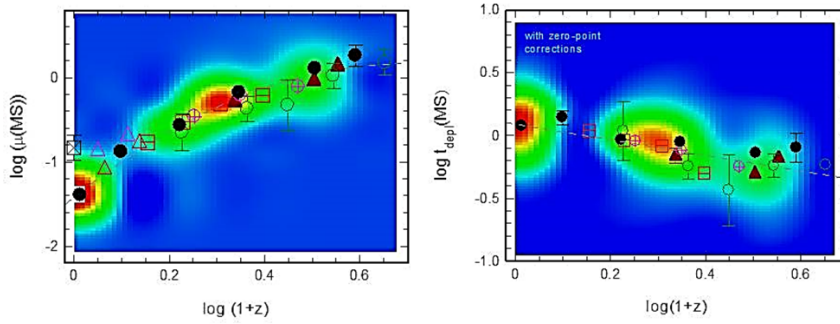


**Fig. 3** Scaling relations of  $\mu_{gas} = M_{molgas}/M_*$  with redshift (left), and depletion time  $t_{dep} = M_{molgas}/\text{SFR}$  (right), for the binned data sets (large symbols) and the individual data points (colored distributions), from Tacconi et al (2018). All available data from NOEMA and ALMA have been taken into account, with zero point corrections. Image reproduced with permission from Tacconi et al (2018), copyright by AAS.

advantage to be completely unbiased by other wavelengths, with the hope to detect brand new objects, obscured in the optical and UV. Both are now described in turn.

#### 4.1 Pointed surveys

Optical/IR surveys have shown that the cosmic star formation density had a peak at about  $z=2$ , and then has dropped by a factor  $\sim 20$  (e.g. Madau and Dickinson, 2014). It was also discovered that, although luminous and ultra-luminous infrared galaxies (ULIRGs) tend to dominate more and more the star formation as  $z$  approaches 1 (Le Floch et al, 2005), the starburst mode is not the dominant star forming mode at  $z \sim 2$ , but contributes only by 10%. The confusion arose at the start because local ULIRGs are all starbursts, due to galaxy interactions and mergers (e.g. Sanders and Mirabel, 1996). Starbursts can be defined as transient states, with an elevated star formation rate (SFR) which cannot be sustained during the "normal" time-scale to consume the gas content of a galaxy, which is 2 Gyr (Bigiel et al, 2008). This time-scale is also called the depletion time  $t_{dep}$ . When the redshift increases, the average SFR increases, and LIRGs or ULIRGs do not require anymore the starburst mode for their interpretation. It is then possible to define a Main Sequence (MS) of "normal" star formation (Whitaker et al, 2012, 2014; Speagle et al, 2014). The specific SFR, divided by the stellar mass, i.e.  $sSFR=SFR/M_*$  increases strongly with redshift, in  $(1+z)^3$  up to  $z \sim 2$ , and decreases only slightly with mass, as  $M_*^{-0.1, -0.4}$  (Lilly et al, 2013). About 90% of the star formation in the Universe occurs on the main sequence, essentially in exponential galaxy disks (e.g. Wuyts et al, 2011).

The evolution of galaxies along the main sequence (MS), and the evolution of the main sequence itself with redshift, have been the object of many models, implying both gas accretion to re-fuel galaxies after the depletion times of the order of a few Gyr, and the moderation of star formation due to the feedback. Some propose a quasi-stationary state (Bouché et al, 2010; Lilly et al, 2013), and others a violent evolution across the MS, passing through a starburst phase or a quiescent one, via violent instabilities and compaction (Dekel et al, 2009; Tacchella et al, 2016).

It is crucial to investigate through the abundance of the molecular component for galaxies on the MS, as a function of redshift, what are the main processes regulating the star formation, and galaxy evolution. A large number of surveys have been carried out, for instance the PHIBSS survey with NOEMA, or the COSMOS with ALMA from dust emission, which demonstrate a large increase of the molecular gas fraction with redshift (Tacconi et al, 2010, 2013; Scoville et al, 2014, 2016), but also a slight decrease of the depletion time, i.e. an increase of star formation efficiency.

In these surveys, two different tracers for the interstellar gas have been used: the most direct one, the CO lines, depending on the CO-to-H<sub>2</sub> conversion factor, and the dust emission in the Rayleigh-Jeans domain, which traces both atomic and molecular gas, but depends also on metallicity, and on the assumed dust temperature, albeit in a linear way (Scoville et al, 2014; Schinnerer et al, 2016). The proportionality factor between dust emission and gas mass is established from nearby galaxies and the Milky Way (through the Planck satellite data), but several parameters may vary, as the slope of the dust opac-

ity with frequency, the metallicity and dust abundance, or the nature of dust. In the literature, it was found that the gas masses derived at high redshift from the dust emission are somewhat larger than that from the CO lines, at least by a factor 2. Part of the explanation could be that dust emission traces both atomic and molecular gas. Although it is very difficult to have direct estimation of the HI gas at high  $z$ , the best estimation comes from the Ly $\alpha$  absorbers along the line of sight towards remote quasars (e.g. Prochaska et al, 2005), and it appears that the cosmic density of HI gas is roughly constant. Given that the molecular gas strongly increases with  $z$ , it is assumed that it will dominate as soon as  $z > 0.5$  (e.g. Lagos et al, 2012).

From a compilation of all literature data on molecular gas at high  $z$ , around the main sequence and slightly above, scaling relations have now been derived for about 1400 objects (Genzel et al, 2015; Tacconi et al, 2018). The main results are a quantification of the increase of gas fraction with  $z$ , and decrease of depletion time, as shown in Fig. 3. These scaling relations take into account all the various parameters (distance from the MS, defined as  $\delta MS = sSFR/sSFR(MS, z, M_*)$ , redshift, stellar mass), exploiting the fact that the dependence of gas fraction and depletion time (or SFE, the Star Formation Efficiency =  $1/t_{dep}$ ) on these parameters is uncorrelated to some extent, i.e. the variables are separable.

The variation of the depletion time with  $\delta MS$  is clear, at a given  $z$  and  $M_*$ ,  $t_{dep}$  is decreasing for galaxies above the MS in the starburst phase, and increasing below in the quenching phase. The main results found by all surveys and analysis is that the gas content in galaxies increases significantly with  $z$ , as  $\sim (1+z)^2$ , but still lower than the SFR on the MS, which is increasing as  $\sim (1+z)^3$  up to  $z=3-4$  (Scoville et al, 2017; Tacconi et al, 2018). In addition, the star formation efficiency (SFE) is increasing with  $z$ , i.e. the depletion time varies as  $(1+z)^{-0.6}$  to  $(1+z)^{-1}$ . There is no dependency of SFE with stellar mass, on the main sequence. The gas fraction, or the gas-to-stellar mass ratio decreases with stellar mass. This explains also the variation of the slope of the MS with stellar mass: if the SFR is almost linear with  $M_*$  for small masses, it then saturates and the slope is lower than 1. Since high mass galaxies have a more massive bulge, and bulges do not participate to star formation, it is tempting to subtract the bulge mass, to check the SFR variation of disk only. Abramson et al (2014) performed the bulge-disk decomposition for large samples of low- $z$  galaxies in the Sloan survey, and indeed, the MS slope is almost vanishing (and vanishes completely in some samples). The sSFR of disks only is quasi independent of their stellar mass. The remaining dependency could be related to the central bulge concentration (Pan et al, 2016).

All these results are supporting models where galaxy evolution and star formation are mainly driven by external gas accretion. Several interpretations have been elaborated (Berta et al, 2013; Scoville et al, 2017). It is possible to trace the evolution of galaxies, their star formation rate and gas content, assuming continuity, neglecting in a first step the contribution of starbursts (5-10%), and the quenched galaxies, which must be of very high mass, and in dense environments (Peng et al, 2010). To maintain the evolution of the MS, it

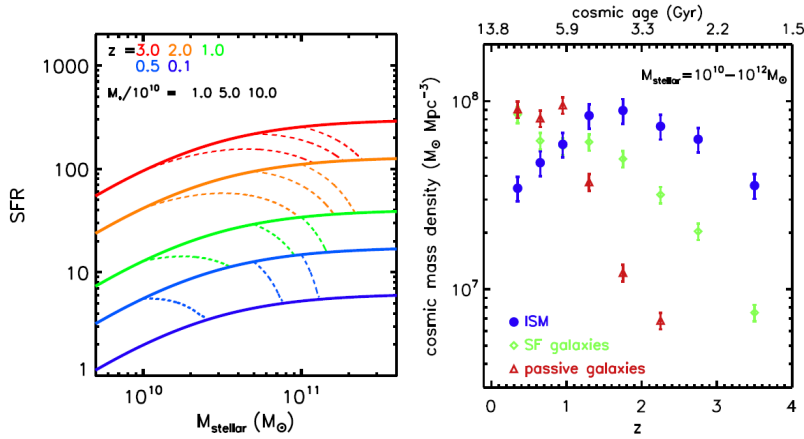


**Fig. 4** *Left:* Evolution of galaxies on the main sequence (MS), assuming they evolve continuously on the MS. The full lines show the MS relations at 5 different redshifts (colours) from the observed consensus compiled by Speagle et al (2014). The dash lines show the time evolution of 1, 5, and  $10 \times 10^{10} M_{\odot}$  galaxies in between two redshifts. They evolve downward and rightward with time, at a rate  $0.7 \text{ SFR}$ , taking into account 30% of stellar mass loss. *Right:* The gas and stellar mass cosmic densities versus redshift for galaxies in the range  $M_{*} = 10^{10}$  to  $10^{12} M_{\odot}$ . These computations have used the observed scaling relations between gas mass and the 3 parameters ( $z$ ,  $\delta\text{MS}$ ,  $M_{*}$ ), and the stellar mass functions from Ilbert et al (2013). Images reproduced with permission from Scoville et al (2017), copyright by AAS.

is necessary that galaxies are continuously accreting gas, to refuel their SFR, given their low depletion time-scales, lower than 1Gyr. This refueling can be mostly due to cold gas accretion (Dekel et al, 2013), but also may include minor mergers. The major mergers are considered to be exceptional events, making galaxies to exit the MS from above for a transient period. Using the empirically determined relations between gas content and SFE with redshift, stellar mass and offset from MS, and assuming  $dM_{*}/dt = 0.7 \text{ SFR}$  (30% of the gas is returned to the interstellar medium through stellar mass loss), it is possible to trace the evolution of individual galaxies on the MS diagram (cf Figure 4). The set of equations can be closed, and the net accretion rates can be derived as a function of  $z$  and the main parameters. For the average considered mass, the accretion rate increases as  $\sim (1+z)^{3.5}$ , which may explain the high SFR in early galaxies, and is justified by the high gas density in the early universe.

Adopting these simplifying hypotheses, and summing over the stellar mass function (e.g. Ilbert et al, 2013), the equations can yield the evolution of the cosmic density of the total gas in galaxies ( $\text{H}_2 + \text{HI}$ , traced by dust emission, result given in Figure 4).

Lensed galaxies allow to explore a lower mass regime ( $M_{*} < 2.5 \cdot 10^{10} M_{\odot}$ ), with lower SFR ( $< 40 M_{\odot}/\text{yr}$ ) (Dessauges-Zavadsky et al, 2015). It is now possible to see the star formation efficiency decrease with stellar mass. This low mass regime reveals the same increase of gas fraction and SFE with redshift.

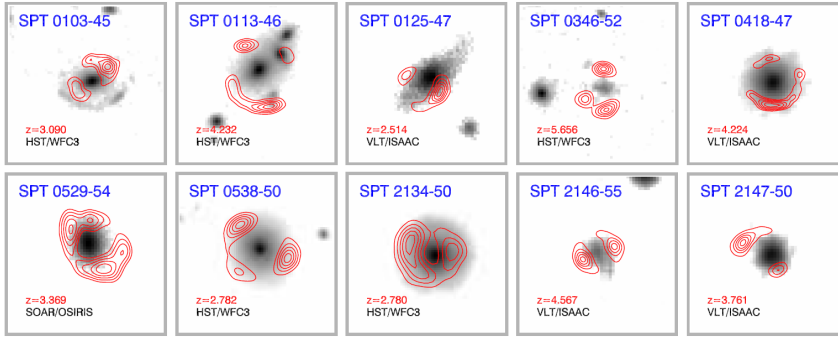


**Fig. 5** ALMA  $870\mu\text{m}$  images of 10 SPT (South Pole Telescope) sources (red contours), superposed on near-infrared images (NIR, grey-scale) from HST, VLT or SOAR telescopes. The NIR indicates the starlight from the foreground lensing galaxies. The high- $z$  galaxies are only seen by ALMA. Their spectroscopic redshifts were determined by ALMA CO line observations, and are shown in red in each panel, of size  $8'' \times 8''$ . Image reproduced with permission from Vieira et al (2013), copyright by Springer.

With both CO lines and dust continuum emission, it is possible to see large variations of the dust-to-gas ratio among the various types of star forming galaxies, even at a given metallicity.

Observations of some gas-rich galaxies below the MS suggests that quenching does not require the total removal or depletion of molecular gas, as many quenching models propose (Suess et al, 2017). Spilker et al (2018) detected with ALMA the CO line in 4 out of 8  $z \sim 0.7$  passive galaxies 3-10 times below the MS. Their gas fraction is below 10%, small enough that the depletion time is rather short. The gas rotation axis is aligned on the stellar one, implying no recent gas accretion. Even though the samples are still not enough to draw firm conclusions, it appears that the quenching towards forming massive red and dead galaxies is rather slow, and due to the cessation of gas accretion.

One of the very successful surveys of ALMA in its first cycle (16 antenna) was to search for CO lines in the high- $z$  ( $z > 1$ ) sample of dusty continuum sources, assembled over 1300 square degrees by the South Pole Telescope (SPT). The survey benefitted from the negative K-correction, and therefore all redshifts were expected with minimum bias. Most of the highest flux sources are lensed. Out of 26 sources, ALMA detected 23 in one CO line (among them 12 with multiple lines, so that the redshift is clearly determined). In the continuum at  $870\mu\text{m}$ , with spatial resolutions  $0.5 - 1.5''$ , only one minute integration per source was sufficient to reveal the arc and ring morphology of the lensed background objects, as displayed in Figure 5. Star formation rates larger than  $500 M_{\odot}/\text{yr}$  imply that the sources are ULIRGs (Vieira et al, 2013). The spectroscopic survey in Band 3 more than doubled the known redshifts at this epoch, and had a median redshift of  $z=3.5$ . The fraction of dusty and luminous starbursts at high  $z$  appears higher than previously thought (see Figure 6).

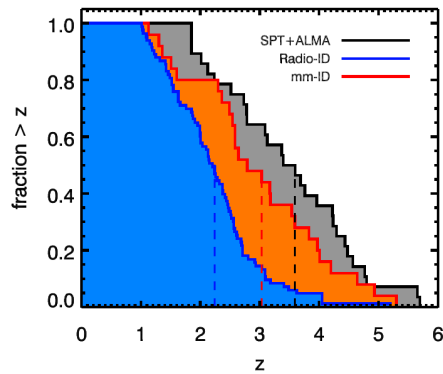


**Fig. 6** The cumulative redshift distribution of luminous, dusty starburst galaxies: the SPT galaxies, with ALMA determined redshifts, are shown in black. The blue sample objects have redshifts determined from rest-frame ultraviolet spectroscopy. The orange sample galaxies in the COSMOS survey have only photometric redshifts from optical/IR. ALMA detected a large fraction of high- $z$  dusty starburst galaxies, and previous surveys were biased to lower redshift than the underlying population. Image reproduced with permission from Vieira et al (2013), copyright by Springer.

#### 4.2 ALMA deep fields

In the UV/optical/IR domains, considerable knowledge on galaxy evolution has come from the study of blank fields, integrating deeply in selected regions of the sky minimizing foregrounds, with the HST (HDF, UDF, XDF, Illingworth et al (2013)), and also with a multitude of instruments at all wavelengths, from the X-ray (Chandra/XMM), to the far-infrared (Spitzer, Herschel) and radio (VLA). From the 11 HST filters, it has been possible to obtain nearly 10 000 photometric redshifts (e.g. Rafelski et al, 2015). Follow-up from the ground has obtained also spectroscopic redshifts, namely with the VLT (Le Fèvre et al, 2004; Bacon et al, 2017), although the latter spectro- $z$  still amount to less than 2% of the total. These surveys have allowed precious knowledge on galaxy properties (sizes, stellar masses, star formation rates), and their evolution with redshift (e.g. Madau and Dickinson, 2014). However, to understand galaxy evolution, the fuel of star formation, the molecular gas, has to be observed. Also optical surveys are biased against the most obscured and dusty star forming galaxies, and sub-mm surveys are needed. Already punctual observations have shown that indeed dusty starbursts exist up to  $z=6$  (Riechers et al, 2013), and surveys with Herschel (Elbaz et al, 2011), or SCUBA-2 (Coppin et al, 2015) have used priors to tackle blending, and stacking to explore just below the sensitivity limit of their instruments.

With ALMA gaining a large factor in sensitivity and spatial resolution, deep surveys are now eagerly expected. The first survey of the Subaru-XMM (SXDF) deep field ( $1.5 \text{ arcmin}^2$  with ALMA) reported by Tadaki et al (2015) has observed in 1.1mm continuum, with a sensitivity of  $\sigma = 55 \mu\text{Jy}/\text{beam}$ . They

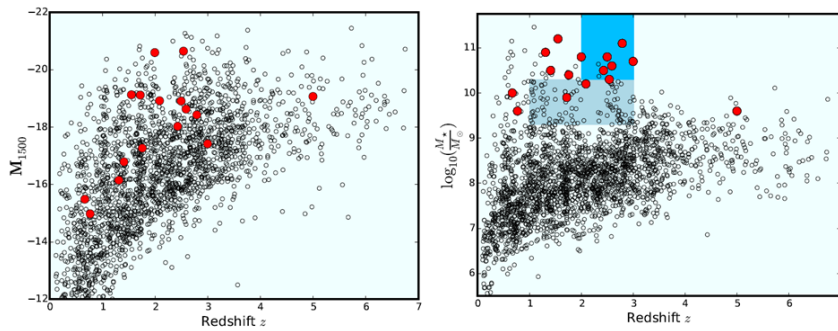


**Fig. 7** *Left:* the UV absolute magnitude of all galaxies in the HUDF, as a function of redshift, with the ALMA 1.3mm detections in red. *Right:* when stellar masses are considered, now the ALMA detections are at the top, meaning that they are indeed the most obscured in UV. The bright blue box emphasizes the ALMA detection of 80% of the most massive galaxies ( $M_* > 2 \cdot 10^{10} M_\odot$ ) at  $z > 2$ . Below  $z=1$ , the detection rate of massive galaxies drops, which indicates possible quenching. The grey-blue box gathers the galaxies which have been stacked and lead to an ALMA global detection. The absence of very massive galaxies above  $z=3$  is clearly visible. Image reproduced with permission from Dunlop et al (2017).

targetted 12 H $\alpha$ -selected star-forming galaxies (SFG) at  $z=2-2.5$ , but detected only 3 of them. The frequency corresponds to 300-400 $\mu\text{m}$  in the rest-frame, so that dust emission should be easy to detect. It also corresponds to 100 $\mu\text{m}$ , the peak of dust emission, for  $z=10$ , and objects with the same mass should be even more easy to detect with the K-correction, so that their absence indicates a drop in the luminosity function with  $z$ . One of the object detected is very compact ( $R_e = 0.7$  kpc), with a high gas fraction of 44%. In the same ALMA field Hatsukade et al (2016) conclude from the possibly detected 23 sources above 0.2mJy that the source count is typical, and comparable to all previous ALMA serendipitous detections.

Dunlop et al (2017) reports about the 4.5 arcmin<sup>2</sup> ALMA survey of the HUDF at 1.3mm at  $\sigma = 30\mu\text{Jy}$  sensitivity. The extraction of reliable sources in continuum is difficult. About 50 sources are first found above  $3.5\sigma$ , but around 30 are also found in negative, i.e. below  $-3.5\sigma$ . Therefore most of the 50 sources must be spurious. Comparing with other data, 16 detections are then secured, through counterparts with HST, infrared and/or radio-cm, 13 of them having a spectroscopic redshift in the optical. The average redshift is  $z=2.15$  and only one source has  $z > 3$ . The lack of high-redshift detections confirms the rapid drop-off of high-mass galaxies in the field, above  $z=3$ . Figure 7 shows clearly that the ALMA detections are among the most UV-obscured objects in the HUDF.

Aravena et al (2016) have carried out a deeper 1.2mm ALMA survey of the HUDF in a restricted region of 1 arcmin<sup>2</sup>, with  $\sigma = 13\mu\text{Jy}$  sensitivity. They detect 9 sources at  $3.5\sigma$  with average  $z=1.6$ , and only one source above  $z=2$ , which is significantly lower than the shallower survey of Dunlop et al (2017). The detections correspond to 55% of the extragalactic background

light (EBL) at 1.2mm measured by the Planck satellite; when stacking all the sources optically known in this region, it is possible to recover 80% of this EBL.

In addition to this continuum survey of 1 arcmin<sup>2</sup> of the HUDF, the same team carried out an ALMA spectroscopic survey (ASPECS, CO and [CII] lines) in two frequency bands at 3mm and 1mm, covering the frequency ranges 84-115 GHz, and 212-272 GHz (Walter et al, 2016). A blind search for lines have found 10 candidates in the 3mm band and 11 at 1mm. The identification of the sources is then done searching for optical/NIR counterparts, with a known redshift. This occurs in 9 out of the 21 candidates. In one or two cases, other CO lines at higher J are also detected in the same survey, and confirm the identification. Most of the times, the lack of other lines suggest that the redshift of the object is large and/or the upper level J of the CO line is large. In addition, stacking has been done for all sources with known redshifts for the first 4 CO lines, but with no detection (Decarli et al, 2016b). Molecular masses were derived for each of the identified sources, and found compatible with previous results for main sequence galaxies, with a large scatter (Decarli et al, 2016a). All results and constraints on the derived cosmic H<sub>2</sub> density are gathered in Figure 8.

From the ASPECS survey, it is now possible to estimate the expected signal from CO lines during an intensity mapping experiment. Based on individual detections only, Carilli et al (2016) estimate the mean surface brightness to 0.94  $\mu$ K at 3mm and 0.55 $\mu$ K at 1.3mm, these values being lower limits to take into account all the possible lines below detection.

## 5 Individual galaxies at high redshift

Besides the large surveys with statistical value to explore galaxy evolution with redshift, the discovery of special cases, pointed observations of high-z quasars, and the study of over-densities, have provided a wealth of information.

### 5.1 Starburst and quasar associations

Objects already known as SMG with single dish continuum detectors were easily detected with ALMA, like this association of three LBG at  $z=5.3$  studied by Riechers et al (2014). From the lines of [CII] and OH detected, an SFR surface density of 530  $M_{\odot}/\text{yr}/\text{kpc}^2$  was derived, implying a disk approaching the Eddington limit for radiation pressure on dust. Since OH is slightly blue-shifted with respect to [CII], this might indicate a molecular outflow due to SN feedback. Swinbank et al (2014) have made a survey with ALMA in the Extended Chandra Deep Field South (ECDFS) of 99 SMG, and found that they are all ULIRGs with SFR  $\sim 300 M_{\odot}/\text{yr}$  and dust temperature of 32K. The contribution of these SMG to the cosmic star formation is about 20% over  $z=1-4$ .

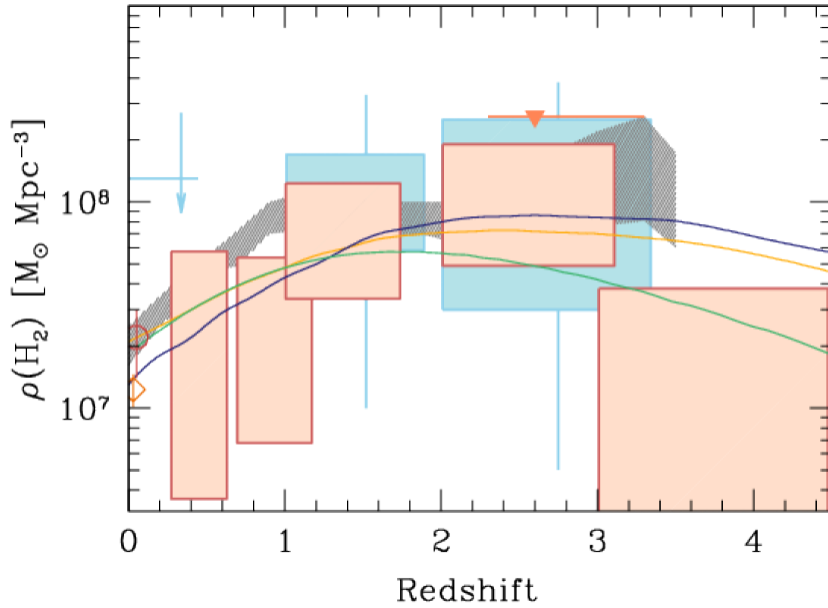


**Fig. 8** Comoving mass density of molecular gas in galaxies  $\rho(\text{H}_2)$  as a function of redshift. The ALMA spectroscopic survey (ASPECS) constraints are plotted in pink boxes, with vertical sizes corresponding to the uncertainties. The blue boxes represent the IRAM interferometer constraints (Walter et al, 2014). The predictions of semi-analytical models are superposed as a yellow line (Obreschkow et al, 2009), a blue line (Lagos et al, 2012) and a green line (Popping et al, 2014). The compilation of literature data on MS galaxies is the grey area (Sargent et al, 2014). The circle symbol at  $z=0$  is from Keres et al (2003), and the losange from Boselli et al (2014). Keating et al (2016) have computed an upper limit (orange triangle) from CO intensity mapping at  $z\sim 3$ . The global behaviour of the  $\text{H}_2$  cosmic density is very similar to the star formation density, with a peak around  $z=2$ . Image reproduced with permission from Decarli et al (2016b), copyright by AAS.

High redshift starbursts can be detected serendipitously, like the bright  $z = 5.24$  lensed submillimeter galaxy in the field of Abell 773 (Combes et al, 2012), as part of the Herschel Lensing Survey (HLS, Egami et al (2010)). This project surveyed a series of nearby galaxy clusters at  $z\sim 0.1-0.5$  playing the role of gravitational telescopes, amplifying background galaxies. These were selected by their very red SPIRE colours, implying a high redshift. Follow-up at millimeter wavelengths allows to discover the spectroscopic redshift, with the help of at least two detected lines. In this case several CO lines up to CO(7-6), CI,  $\text{H}_2\text{O}$  and the [NII]205 $\mu\text{m}$  lines were discovered, and allowed to constrain the variations of fundamental constants (Levshakov et al, 2012). With ALMA, spectroscopic redshifts are obtained routinely.

An hyperluminous quasar at  $z=4.4$  selected from WISE-SDSS was detected with ALMA by Bischetti et al (2018) in dust continuum and [CII] line. It is at the center of a proto-cluster, merging with two close companions. The quasar is actively forming stars with  $\text{SFR} \sim 100 M_\odot/\text{yr}$ , and the host galaxy

will increase its stellar mass more rapidly than its black hole mass, which is observed 2 orders of magnitude too massive, with respect to local relations.

Venemans et al (2017) have detected several CO lines, CI and [CII] in  $z \sim 7$  quasars, and shown that these lines have excitation compatible with photodissociation regions, but not X-ray dominated regions. The properties of the molecular gas and dust in these quasars are dominated by an important star-formation activity, confirming that intense starbursts are co-existing with AGN activities.

## 5.2 Lensed high- $z$ galaxies, high spatial resolution and GMC studies

ALMA can have very high spatial resolution in its extended configuration, up to 15-20 milli-arcsec (mas). A remarkable object was observed to demonstrate these capabilities, with baselines up to 15km: SDP.81 (ALMA Partnership et al, 2015). This gravitationally lensed galaxy at  $z=3.042$  was discovered by the Herschel survey H-ATLAS (Eales et al, 2010; Negrello et al, 2010). Its redshift was determined through CO lines; the lensing galaxy is at  $z = 0.299$ , and the amplification factor is  $\mu = 11$  (Bussmann et al, 2013). With a beam of 25mas at 1mm (180pc at  $z=3.042$ ), the ALMA continuum map reveals the two gravitational arcs with unprecedented sharpness. Figure 9 show a tapered version of the maps in continuum, CO and H<sub>2</sub>O lines; the images have been tapered to lower resolution to gain more signal to noise. The two arcs are part of an Einstein ring, of radius 1.5". The foreground lensing galaxy is invisible on these images, except for a weak continuum source at the center of the ring, which has a spectral index consistent with synchrotron emission. The lensing galaxy is a massive elliptical ( $3.6 \cdot 10^{11} M_{\odot}$  inside the Einstein ring of 1.5" = 6.7 kpc, at  $z=0.299$ , and no AGN is detected optically. But the 1.4 GHz flux is compatible with the mm spectral index, and corresponds to an AGN radio core. The continuum from the arcs comes from dust emission in the high- $z$  star forming galaxy, with an SFR = 527  $M_{\odot}/\text{yr}$ . The three CO lines detected (from J=5, 8 and 10) show regions in the galaxy of different excitation, implying a complex structure. The H<sub>2</sub>O emission comes from a thermal line, which ratio with the CO lines is rather weak, may be due to differential lensing. The wealth of details acquired in  $\sim 30$ h of telescope time in early science with only 22 to 36 antennae is quite impressive.

Given the enhanced spatial resolution due to lensing, it is possible to explore the resolved Kennicutt-Schmidt relation (KS) in these high- $z$  galaxies. The surface densities of the molecular gas and star formation rate have been compared in different regions of SDP.81 ( $z \sim 3$ ) (Sharda et al, 2018). There is much more SFR than predicted from the linear KS relation, and the authors propose another relation between gas and SFR, taking into account the free-fall time of the clouds. Since the observed turbulence in the cloud is much higher than for local galaxies, based on the observed high gas velocity dispersion, a model of multifreefall based on turbulence (Salim et al, 2015) is in better agreement with observations. Note that another attempt to derive the

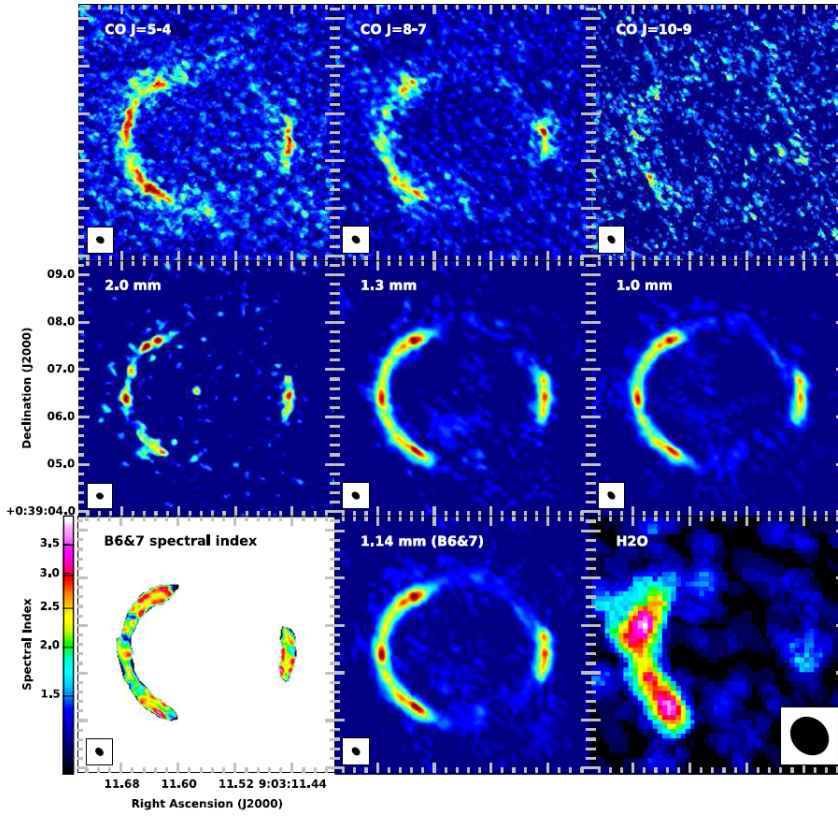


**Fig. 9** ALMA images with high resolution (CO lines and continuum, 100-170mas) or lower resolution ( $\text{H}_2\text{O}$  line, 900mas). *Top*: CO  $J = 5-4$ ,  $8-7$ , and  $10-9$  integrated intensity. *Middle*: 2.0, 1.3, and 1.0 mm continuum. *Bottom*: Band 6 and 7 spectral index, 1.14 mm continuum (combined Band 6 and 7 data), and  $\text{H}_2\text{O}$  integrated intensity. The beam sizes are indicated by the black ellipses at the bottom of the panels. Image reproduced with permission from ALMA Partnership et al (2015), copyright by AAS.

resolved KS relation for distant galaxies, even without any lensing, has given results compatible with the linear KS relation (Freundlich et al, 2013).

ALMA is now able to detect normal galaxies at  $z \sim 7$  (e.g. Maiolino et al, 2015). With the [CII] line and continuum dust emission, the detection of Lyman break galaxies have been successful, implying SFR of  $5-15 M_{\odot}/\text{yr}$ . A spatial offset of the order of 4 kpc has been observed between the [CII] emission and the  $\text{Ly}\alpha$  line and far UV, suggesting that stellar feedback rapidly destroys/disperses the molecular clouds.

### 5.3 Black hole mass estimation at high- $z$

A large number of quasars have been detected now at  $z \sim 6$  in molecules, and their CO/[CII] kinematics can be used to derive the central dynamical mass. From their broad lines detected in optical, and a widely known relation between Broad Line Region (BLR) luminosity and radius calibrated from reverberation mapping (e.g. Bentz et al, 2013), it is possible to compare the black hole mass ( $M_{BH}$ ), and the host dynamical mass. The high- $z$  quasars appear all with a much higher black-hole mass than expected from their dynamical mass and the local  $M$ - $\sigma$  relation (Wang et al, 2013; Venemans et al, 2016). This surprising result could come from the large uncertainties of the mass estimation. It is not possible to distinguish bulge and disk, so the  $M_{BH}$  is compared to the total host dynamical mass, but this is precisely conservative. The inclination of the rotating molecular disk is not well known, and the result is valid only statistically. The  $M_{BH}$  estimation has also a fudge factor for inclination. In most systems, it is assumed that the [CII] or CO lines are centered on the systemic velocity, and can be reliably used to derive the dynamical mass of the central stellar bulge. However, the optical MgII broad emission lines are systematically blue-shifted. The average blue-shift is of  $\sim 500$  km/s, but can be found up to 1700 km/s. This is interpreted as an outflow due to the central AGN, given that the symmetrical red-shifted region behind is too obscured to be seen.

Even if the dynamical mass is not well estimated, it is possible to have a lower limit for it with the mass of the gas, estimated from both the lines and the dust emission. In these high- $z$  systems, the gas fraction is often larger than 50%, and the dynamical mass cannot be more underestimated than by a factor 2. The derived black hole masses are then robustly 3-4 higher than expected from the local relation (see Figure 10).

### 5.4 Ly-alpha blobs and proto-clusters

Protoclusters are overdensities in the early universe, where the growth of structures and their accompanying black holes are accelerated. They are not yet virialised into clusters, but are precious to understand why black holes might start growing very quickly, and AGN feedback might shape the first galaxies. Narrowband imaging at rest-frame Ly- $\alpha$  have revealed accumulation of Ly- $\alpha$  emitters (LAE), but also extended ( $>30$  kpc) Ly- $\alpha$  emission (often termed Lyman-Alpha Blobs, LAB) (e.g. Steidel et al, 2000; Matsuda et al, 2004). In these protoclusters, X-ray observations have revealed a significantly higher (by a factor  $\sim 5$ ) fraction of AGN (e.g. Lehmer et al, 2009), suggesting a longer duty-cycle for black hole accretion in galaxies of rich environments. Alexander et al (2016) observed with ALMA such AGN in proto-clusters and obtained a high detection rate, implying SFRs of 200-400  $M_{\odot}/\text{yr}$ , somewhat enhanced with respect to the field. This enhanced star formation may explain the ex-

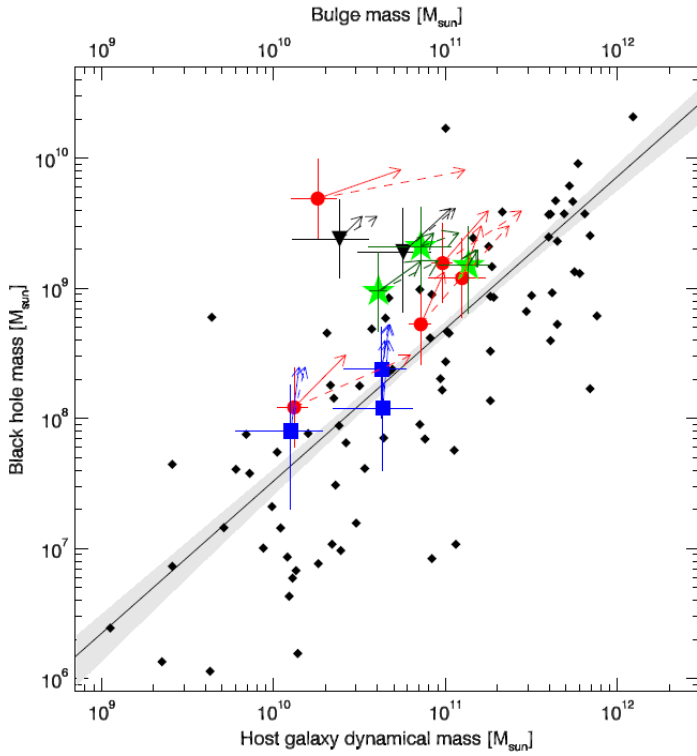


**Fig. 10** Black hole mass versus the dynamical mass of  $z \sim 6$  quasar host galaxies and the bulge mass of local galaxies. The black diamonds are values obtained for local galaxies (Kormendy and Ho, 2013). Their  $M_{BH} - M_{bulge}$  relation is represented by the solid line and the shaded area. The large and colored symbols are the high- $z$  quasars. The green stars are the  $z > 6.5$  quasars from Venemans et al (2016). For a given bulge mass, the high-redshift quasars have a more massive black hole than local galaxies. From the quasar luminosity (linked to its accretion rate), and from the observed star formation rate, it is possible to extrapolate the trajectory of the points (arrows) during the next 50 Myr. Image reproduced with permission from Venemans et al (2016), copyright by AAS.

tended Ly- $\alpha$  emission of the LAB, given a reasonable escape fraction for the continuum ionizing photons.

Proto-clusters can also be the site of a colder gas phase, which is extended as a circumgalactic medium (CGM) around the main galaxies. A striking example is the Spiderweb, a conglomerate of merging galaxies at  $z=2.2$  (Emonts et al, 2016). Several CO lines and CI were observed with ALMA and ATCA, showing an extended network of clumps and filaments, with gas excitation similar to that of the Milky Way (see Figure 11). The gas is metal enriched and dense, and most of it must come from tidal and ram-pressure stripping from the interacting/merging galaxies in the central region of the proto-cluster (Emonts et al, 2018).

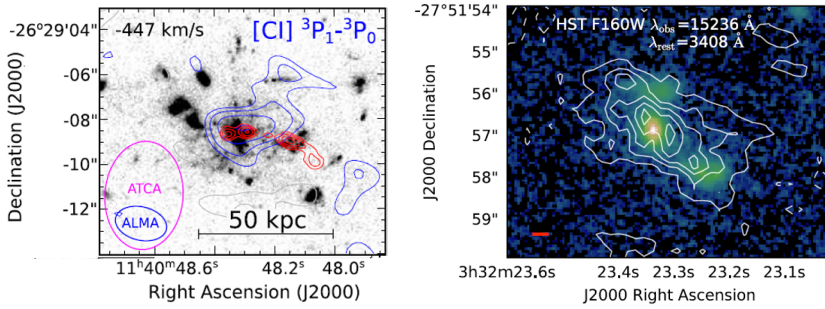


**Fig. 11** *Left*: One channel map ( $V=-447\text{km/s}$ ,  $90\text{km/s}$  wide) of the [CI] emission obtained with ALMA towards the Spiderweb proto-cluster of galaxies (Emonts et al, 2018). The blue contours are from [CI] $^3\text{P}_1\text{-}^3\text{P}_0$  emission, and the red contours from the 36 GHz radio continuum, both overlaid on the HST image. *Right*: Overlay of CO(4-3) contours on the HST F160W image of the Candels-5001 proto-cluster at  $z=3.47$  (Ginolfi et al, 2017). The red bar is the HST PSF, at  $0.34\mu\text{m}$  in the rest frame. Images reproduced with permission from Emonts et al (2018) and Ginolfi et al (2017).

Molecular gas structures elongated on scales of  $\sim 40$  kpc are not rare in high- $z$  proto-clusters, and a molecular mass of  $2\text{-}6 \cdot 10^{11} M_{\odot}$  has been detected in CO(4-3) and dust emission, with clumping and relatively high metallicity, at  $z=3.5$  (Ginolfi et al, 2017). The extended structure is compatible with a tidal/ram pressure origin, but could also be fueled by some cold gas accretion (see Figure 11).

## 6 Epoch of reionization

Stark (2016) has reviewed our knowledge of early galaxies, in the first billion years after the Big-Bang. For  $z>6$ , ALMA yields a good opportunity to detect the dust emission, provided that they are dusty enough. The peak of dust emission is indeed shifted towards  $\lambda > 0.7\text{mm}$ . For high- $z$  objects, it becomes difficult to obtain spectroscopic redshifts optically, especially when obscured by dust. ALMA can then help to identify the objects, thanks to the [CII] line at  $158\mu\text{m}$ , redshifted to  $\lambda > 1.1\text{mm}$ . Models of the ISM had predicted that the main coolant would be through this [CII] line, however the observations reserved some surprises. The photoelectric heating efficiency of the dust, measured by the ratio  $L_{[\text{CII}]} / L_{\text{FIR}}$ , varies by about 2 orders of magnitude, and is decreasing at high  $L_{\text{FIR}}$ , for strong starbursts. The main factor reducing this efficiency has been shown to be the dust temperature, and the strong UV field (Malhotra et al, 2017): indeed, the  $L_{[\text{CII}]} / L_{\text{FIR}}$  ratio is very well anti-correlated to the dust temperature, whatever the redshift. Figure 12 gathers a large fraction of the [CII] studies so far, and shows that the [CII]/FIR ratio is higher at high redshift, although still declining with  $L_{\text{FIR}}$ . The high- $z$  quasars detected reveal a wide range of properties, sometimes behaving like starbursts, while sometimes the quasar excitation may prevail (e.g. Venemans et al, 2016).

Many searches have been made with ALMA, with some surprising failures, indicating that galaxies are really "primordial", with low metallicity ( $Z < 0.1$ ) and little dust. The typical Ly $\alpha$  emitter Himiko was not detected in the continuum, nor in the [CII] line (Ouchi et al, 2013). Several other upper limits confirmed that most LBG between  $z=6$  and 8 are very difficult to detect, even with gravitational lensing (e.g. Schaerer et al, 2015). With more observations, Himiko is now detected in the [CII] line, but not in dust emission (Carniani et al, 2018), revealing a dust deficiency.

Evidence also exists of early galaxies, with their ISM extended over kpc sizes, but weak or undetected in dust emission, while revealing strong [CII] line emission (Capak et al, 2015). These show some similarity to low-metallicity dwarfs in the local Universe, like the LMC, which have a very high  $L_{[CII]}/L_{FIR}$  ratio. However, these high- $z$  objects are much more massive, which implies on the contrary a rapid evolution in the ISM dust properties over redshift, due to metal deficiency. Selecting their objects with a relatively lower Ly $\alpha$  equivalent widths, indicating the presence of dust, at a given UV luminosity, Willott et al (2015) reports dust emission and [CII] line detections at  $z \sim 6$ . The velocity redshift of the Ly $\alpha$  with respect to the [CII] line is very prominent at high- $z$ , due to increased intergalactic gas (IGM) absorption of the blue wing of Ly $\alpha$ . The expected enhancement of IGM absorption in the EoR, is not always there (Pentericci et al, 2016), implying patchy reionization.

At high- $z$ , galaxies are clumpy, and sometimes the [CII] line and even the [OIII] line at  $88\mu\text{m}$  are spatially offset from the Ly $\alpha$  or UV clumps (Carniani et al, 2017; Matthee et al, 2017). These offsets may be explained by obscuration, different excitation or metallicity of the different tracers. Alternatively, strong feedback could have removed a large fraction of gas and dust, or several parts of the systems are interacting while assembling, as suggested by theoretical models (Katz et al, 2017).

Some of the highest redshifts found in the EoR with ALMA are the  $z=8.38$  gravitationally lensed galaxy selected from deep HST imaging in the Frontier Field cluster Abell 2744 (Laporte et al, 2017), or the Lyman Break galaxy at  $z=8.31$  behind the Frontier Field cluster MACS J0416.1-2403 (Tamura et al, 2018). Dust emission and the [OIII] line have been detected, raising the problem of forming such dust amounts  $\sim 600$  Myr after the Big Bang. This would imply that each SN-II explosion has been able to produce  $0.5 M_{\odot}$  of dust, during the  $\text{SFR}=15\text{-}20 M_{\odot}/\text{yr}$  star forming phase, since  $z=10\text{-}12$ .

The highest redshift is MACS1149-JD1 at  $z=9.11$ , a lensed galaxy detected in the [OIII] line. No redshift was known from the optical before, and the [OIII] line was used to measure the redshift. The colors of its stellar population show that star formation began at  $z=15$  in this galaxy (Hashimoto et al, 2018).

Contrary to many ALMA surveys, finding a drop in their source number at high redshift, Strandet et al (2016) find a redshift distribution much more weighted towards the high- $z$ , because of a low-frequency selection. Dusty sources were selected from the South Pole Telescope (SPT) survey, from their

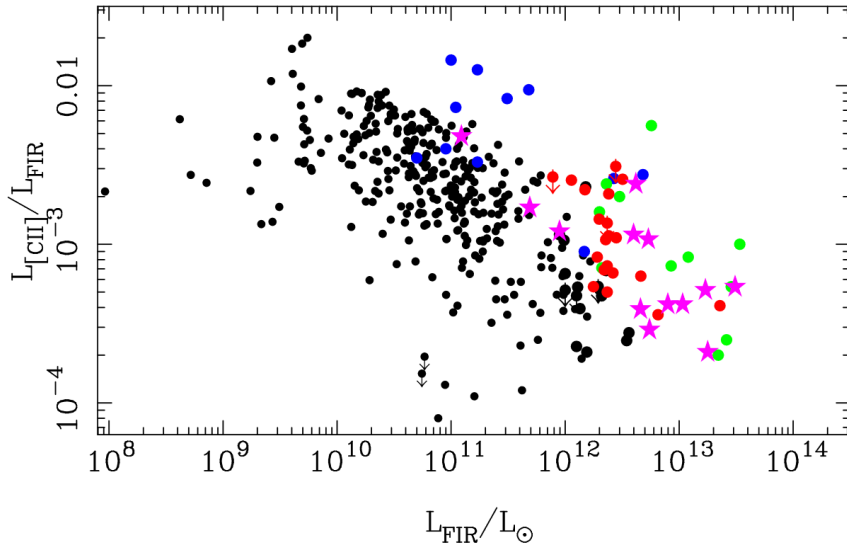


**Fig. 12** The [CII] to FIR luminosity ratio versus the FIR luminosity. The low-redshift galaxies are plotted as black circles, from Malhotra et al (2001), Luhman (2013), and Díaz-Santos et al (2013). Various ULIRGs at high redshift ( $z=1$  to 6) detections from the literature are in green circles, and the Hello sources ( $z=1-3$ ) amplified by lenses are in blue circles (Malhotra et al, 2017). The red circles are the high- $z$  SPT sources from Gullberg et al (2015), corrected for their amplification factor. Quasars at  $z>4$  are plotted as magenta stars (Venemans et al, 2012, 2016). At high  $z$ , the [C II]/FIR ratio still declines with FIR luminosity, but takes higher values than at  $z=0$ .

1.4mm continuum flux; eliminating the synchrotron sources, by requiring 1.4mm flux being twice higher than the 2mm flux.

Although most of high- $z$  star forming objects selected optically have low dust content, exceptional objects exist, like HFLS3, at  $z=6.34$ , with  $\text{SFR}=2900 M_{\odot}/\text{yr}$ , a gas mass of  $10^{11} M_{\odot}$ , including  $2 \cdot 10^{11} M_{\odot}$  of atomic gas, and a depletion time of 36 Myr (Riechers et al, 2013). These must be located in proto-clusters, and are the progenitors of massive ellipticals in clusters today.

## 7 Summary

ALMA has been working now for about 7 years since its commissioning in 2011, and has accumulated a wealth of data, which have yet to be digested and interpreted. In many domains, ALMA has provided impressive breakthroughs, with unprecedented sensitivity and spatial resolution.

One of the main goals in galaxy evolution is to determine the molecular gas properties of galaxies as a function of redshift, to better understand the cosmic star formation history. This has been done through pointed observations, with large sample of objects selected from their stellar mass and SFR, being on the main sequence of star forming galaxies, where are born 90% of the stars in the

Universe. Two main factors have been emphasized: the gas fraction increases steadily on the main sequence, as  $(1+z)^2$ , and this is the main reason of the peak in the SFRD at  $z \sim 2$ . At a lower level, the star formation efficiency is also increasing with redshift, as  $(1+z)^\alpha$ , with  $\alpha=0.6-1$ , (or the depletion time is decreasing, as  $(1+z)^{-\alpha}$ ), although the cause of this has not been clearly identified: either due to smaller and denser galaxies, with a shorter dynamical time, or due to a larger importance of galaxy interactions. Although some galaxy molecular maps have been done, and resolved Kennicutt-Schmidt relation explored, this is only the beginning, and the influence of morphology, kinematics and dynamics of galaxies is not yet understood.

In parallel, deep blind surveys, completely unbiased by previous wavelengths, have been carried out focussed either on the dust continuum, or the CO lines, with shallow or deeper approaches, according to the surface covered. The hope was to detect dusty galaxies at very high redshift, not suspected by other surveys. Eventually, dusty and massive galaxies are not as frequent as previously hoped at  $z$  larger than 5, which confirms the high- $z$  drop in optical surveys. ALMA is now opening clearly the windows of the epoch of re-ionization, and it is likely that the main actors to reionize the Universe will turn out to be a large number of small and dwarf galaxies, while the major starbursts and quasars have a minor influence.

ALMA surveys have begun to unveil the cosmic evolution of the  $H_2$  content, but this is only the beginning, with huge error-bars, not allowing to disentangle the various theoretical models, as shown in Figure 8. In the future, this cosmic evolution will be compared with the star formation history, and also with the atomic gas content, to have a more precise budget of gas and star formation at all epochs.

There remain a large number of unsolved issues, like the symbiotic evolution of black hole and bulges in galaxies, which appear to be divergent at high redshift, the importance of AGN feedback in the early universe, the influence of environment in proto-clusters. The detection of important quantities of cold and dense gas in the circumgalactic medium at early times might give some clues in the missing baryon problem.

**Acknowledgements** I thank Paul Ho for inviting me to write this review.

## References

- Abramson LE, Kelson DD, Dressler A, Poggianti B, Gladders MD, Oemler A Jr, Vulcani B (2014) The Mass-independence of Specific Star Formation Rates in Galactic Disks. *ApJ*785:L36, DOI 10.1088/2041-8205/785/2/L36, 1402.7076
- Alexander DM, Simpson JM, Harrison CM, Mullaney JR, Smail I, Geach JE, Hickox RC, Hine NK, Karim A, Kubo M, Lehmer BD, Matsuda Y, Rosario DJ, Stanley F, Swinbank AM, Umehata H, Yamada T (2016) ALMA observations of a  $z \sim 3.1$  protocluster: star formation from active galactic nuclei

- and Lyman-alpha blobs in an overdense environment. *MNRAS*461:2944–2952, DOI 10.1093/mnras/stw1509, 1601.00682
- ALMA Partnership, Vlahakis C, Hunter TR, Hodge JA, Pérez LM, Andreani P, Brogan CL, Cox P, Martin S, Zwaan M, Matsushita S, Dent WRF, Impellizzeri CMV, Fomalont EB, Asaki Y, Barkats D, Hills RE, Hirota A, Kneissl R, Liuzzo E, Lucas R, Marcelino N, Nakanishi K, Phillips N, Richards AMS, Toledo I, Aladro R, Broguiere D, Cortes JR, Cortes PC, Espada D, Galarza F, Garcia-Appadoo D, Guzman-Ramirez L, Hales AS, Humphreys EM, Jung T, Kamenno S, Laing RA, Leon S, Marconi G, Mignano A, Nikolic B, Nyman LA, Radiszcz M, Remijan A, Rodón JA, Sawada T, Takahashi S, Tilanus RPJ, Vila Vilaro B, Watson LC, Wiklind T, Ao Y, Di Francesco J, Hatsukade B, Hatziminaoglou E, Mangum J, Matsuda Y, van Kampen E, Wootten A, de Gregorio-Monsalvo I, Dumas G, Francke H, Gallardo J, Garcia J, Gonzalez S, Hill T, Iono D, Kaminski T, Karim A, Krips M, Kurono Y, Lonsdale C, Lopez C, Morales F, Plarre K, Videla L, Villard E, Hibbard JE, Tatematsu K (2015) The 2014 ALMA Long Baseline Campaign: Observations of the Strongly Lensed Submillimeter Galaxy HATLAS J090311.6+003906 at  $z = 3.042$ . *ApJ*808:L4, DOI 10.1088/2041-8205/808/1/L4, 1503.02652
- Aravena M, Decarli R, Walter F, Da Cunha E, Bauer FE, Carilli CL, Daddi E, Elbaz D, Ivison RJ, Riechers DA, Smail I, Swinbank AM, Weiss A, Anguita T, Assef RJ, Bell E, Bertoldi F, Bacon R, Bouwens R, Cortes P, Cox P, González-López J, Hodge J, Ibar E, Inami H, Infante L, Karim A, Le Le Fèvre O, Magnelli B, Ota K, Popping G, Sheth K, van der Werf P, Wagg J (2016) The ALMA Spectroscopic Survey in the Hubble Ultra Deep Field: Continuum Number Counts, Resolved 1.2 mm Extragalactic Background, and Properties of the Faintest Dusty Star-forming Galaxies. *ApJ*833:68, DOI 10.3847/1538-4357/833/1/68, 1607.06769
- Bacon R, Conseil S, Mary D, Brinchmann J, Shepherd M, Akhlaghi M, Weilbacher PM, Piqueras L, Wisotzki L, Lagattuta D, Epinat B, Guerou A, Inami H, Cantalupo S, Courbot JB, Contini T, Richard J, Maseda M, Bouwens R, Bouché N, Kollatschny W, Schaye J, Marino RA, Pello R, Herenz C, Guiderdoni B, Carollo M (2017) The MUSE Hubble Ultra Deep Field Survey. I. Survey description, data reduction, and source detection. *A&A*608:A1, DOI 10.1051/0004-6361/201730833, 1710.03002
- Bentz MC, Denney KD, Grier CJ, Barth AJ, Peterson BM, Vestergaard M, Bennert VN, Canalizo G, De Rosa G, Filippenko AV, Gates EL, Greene JE, Li W, Malkan MA, Pogge RW, Stern D, Treu T, Woo JH (2013) The Low-luminosity End of the Radius-Luminosity Relationship for Active Galactic Nuclei. *ApJ*767:149, DOI 10.1088/0004-637X/767/2/149, 1303.1742
- Berta S, Lutz D, Nordon R, Genzel R, Magnelli B, Popesso P, Rosario D, Saintonge A, Wuyts S, Tacconi LJ (2013) Molecular gas mass functions of normal star-forming galaxies since  $z \sim 3$ . *A&A*555:L8, DOI 10.1051/0004-6361/201321776, 1304.7771
- Bigiel F, Leroy A, Walter F, Brinks E, de Blok WJG, Madore B, Thornley MD (2008) The Star Formation Law in Nearby Galaxies on Sub-Kpc Scales.

- AJ136:2846–2871, DOI 10.1088/0004-6256/136/6/2846, 0810.2541
- Bischetti M, Piconcelli E, Feruglio C, Duras F, Bongiorno A, Carniani S, Marconi A, Pappalardo C, Schneider R, Travascio A, Valiante R, Vietri G, Zappacosta L, Fiore F (2018) The WISSH quasars project V. ALMA reveals the assembly of a giant galaxy around a  $z=4.4$  hyper-luminous QSO. ArXiv e-prints 1804.06399
- Blain AW, Smail I, Ivison RJ, Kneib JP, Frayer DT (2002) Submillimeter galaxies. Phys. Rep.369:111–176, DOI 10.1016/S0370-1573(02)00134-5, astro-ph/0202228
- Bolatto AD, Wolfire M, Leroy AK (2013) The CO-to-H<sub>2</sub> Conversion Factor. ARA&A51:207–268, DOI 10.1146/annurev-astro-082812-140944, 1301.3498
- Boselli A, Cortese L, Boquien M, Boissier S, Catinella B, Lagos C, Saintonge A (2014) Cold gas properties of the Herschel Reference Survey. II. Molecular and total gas scaling relations. A&A564:A66, DOI 10.1051/0004-6361/201322312, 1401.8101
- Bouché N, Dekel A, Genzel R, Genel S, Cresci G, Förster Schreiber NM, Shapiro KL, Davies RI, Tacconi L (2010) The Impact of Cold Gas Accretion Above a Mass Floor on Galaxy Scaling Relations. ApJ718:1001–1018, DOI 10.1088/0004-637X/718/2/1001, 0912.1858
- Brown RL, Vanden Bout PA (1992) IRAS F10214 + 4724 - an extended CO emission source at  $Z = 2.2867$ . ApJ397:L19–L22, DOI 10.1086/186534
- Bussmann RS, Pérez-Fournon I, Amber S, Calanog J, Gurwell MA, Dannerbauer H, De Bernardis F, Fu H, Harris AI, Krips M, Lapi A, Maiolino R, Omont A, Riechers D, Wardlow J, Baker AJ, Birkinshaw M, Bock J, Bourne N, Clements DL, Cooray A, De Zotti G, Dunne L, Dye S, Eales S, Farrah D, Gavazzi R, González Nuevo J, Hopwood R, Ibar E, Ivison RJ, Laporte N, Maddox S, Martínez-Navajas P, Michalowski M, Negrello M, Oliver SJ, Roseboom IG, Scott D, Serjeant S, Smith AJ, Smith M, Streblyanska A, Valiante E, van der Werf P, Verma A, Vieira JD, Wang L, Wilner D (2013) Gravitational Lens Models Based on Submillimeter Array Imaging of Herschel-selected Strongly Lensed Sub-millimeter Galaxies at  $z > 1.5$ . ApJ779:25, DOI 10.1088/0004-637X/779/1/25, 1309.0836
- Capak PL, Carilli C, Jones G, Casey CM, Riechers D, Sheth K, Carollo CM, Ilbert O, Karim A, Lefevre O, Lilly S, Scoville N, Smolcic V, Yan L (2015) Galaxies at redshifts 5 to 6 with systematically low dust content and high [C II] emission. Nature522:455–458, DOI 10.1038/nature14500, 1503.07596
- Carilli CL, Walter F (2013) Cool Gas in High-Redshift Galaxies. ARA&A51:105–161, DOI 10.1146/annurev-astro-082812-140953, 1301.0371
- Carilli CL, Chluba J, Decarli R, Walter F, Aravena M, Wagg J, Popping G, Cortes P, Hodge J, Weiss A, Bertoldi F, Riechers D (2016) The ALMA Spectroscopic Survey in the Hubble Ultra Deep Field: Implications for Spectral Line Intensity Mapping at Millimeter Wavelengths and CMB Spectral Distortions. ApJ833:73, DOI 10.3847/1538-4357/833/1/73, 1607.06773
- Carniani S, Maiolino R, Pallottini A, Vallini L, Pentericci L, Ferrara A, Castel-

- lano M, Vanzella E, Grazian A, Gallerani S, Santini P, Wagg J, Fontana A (2017) Extended ionised and clumpy gas in a normal galaxy at  $z = 7.1$  revealed by ALMA. *A&A*605:A42, DOI 10.1051/0004-6361/201630366, 1701.03468
- Carniani S, Maiolino R, Smit R, Amorín R (2018) ALMA Detection of Extended [C II] Emission in Himiko at  $z=6.6$ . *ApJ*854:L7, DOI 10.3847/2041-8213/aaab45, 1712.01890
- Casey CM, Narayanan D, Cooray A (2014) Dusty star-forming galaxies at high redshift. *Phys. Rep.*541:45–161, DOI 10.1016/j.physrep.2014.02.009, 1402.1456
- Chapman SC, Blain AW, Smail I, Ivison RJ (2005) A Redshift Survey of the Submillimeter Galaxy Population. *ApJ*622:772–796, DOI 10.1086/428082, [astro-ph/0412573](#)
- Combes F (2008) Molecular absorptions in high- $z$  objects. *Ap&SS*313:321–326, DOI 10.1007/s10509-007-9632-3, [astro-ph/0701894](#)
- Combes F, Maoli R, Omont A (1999) CO lines in high redshift galaxies: perspective for future MM instruments. *A&A*345:369–379, [astro-ph/9902286](#)
- Combes F, Rex M, Rawle TD, Egami E, Boone F, Smail I, Richard J, Ivison RJ, Gurwell M, Casey CM, Omont A, Berciano Alba A, Dessauges-Zavadsky M, Edge AC, Fazio GG, Kneib JP, Okabe N, Pelló R, Pérez-González PG, Schaerer D, Smith GP, Swinbank AM, van der Werf P (2012) A bright  $z = 5.2$  lensed submillimeter galaxy in the field of Abell 773. *HLSJ*091828.6+514223. *A&A*538:L4, DOI 10.1051/0004-6361/201118750, 1201.2908
- Coppin KEK, Geach JE, Almaini O, Arumugam V, Dunlop JS, Hartley WG, Ivison RJ, Simpson CJ, Smith DJB, Swinbank AM, Blain AW, Bourne N, Bremer M, Conzelmann C, Harrison CM, Mortlock A, Chapman SC, Davies LJM, Farrah D, Gibb A, Jenness T, Karim A, Knudsen KK, Ibar E, Michałowski MJ, Peacock JA, Rigopoulou D, Robson EI, Scott D, Stevens J, van der Werf PP (2015) The SCUBA-2 Cosmology Legacy Survey: the submillimetre properties of Lyman-break galaxies at  $z = 3-5$ . *MNRAS*446:1293–1304, DOI 10.1093/mnras/stu2185, 1407.6712
- Cox P (2005) Molecular Gas at High Redshift. In: Lis DC, Blake GA, Herbst E (eds) *Astrochemistry: Recent Successes and Current Challenges*, IAU Symposium, vol 231, pp 291–300, DOI 10.1017/S1743921306007289
- da Cunha E, Groves B, Walter F, Decarli R, Weiss A, Bertoldi F, Carilli C, Daddi E, Elbaz D, Ivison R, Maiolino R, Riechers D, Rix HW, Sargent M, Smail I (2013) On the Effect of the Cosmic Microwave Background in High-redshift (Sub-)millimeter Observations. *ApJ*766:13, DOI 10.1088/0004-637X/766/1/13, 1302.0844
- David LP, Lim J, Forman W, Vrtiljek J, Combes F, Salome P, Edge A, Hamer S, Jones C, Sun M, O’Sullivan E, Gastaldello F, Bardelli S, Temi P, Schmitt H, Ohyama Y, Mathews W, Brighenti F, Giacintucci S, Trung DV (2014) Molecular Gas in the X-Ray Bright Group NGC 5044 as Revealed by ALMA. *ApJ*792:94, DOI 10.1088/0004-637X/792/2/94, 1407.3235
- Decarli R, Walter F, Aravena M, Carilli C, Bouwens R, da Cunha E, Daddi E,

- Elbaz D, Riechers D, Smail I, Swinbank M, Weiss A, Bacon R, Bauer F, Bell EF, Bertoldi F, Chapman S, Colina L, Cortes PC, Cox P, González-López J, Inami H, Ivison R, Hodge J, Karim A, Magnelli B, Ota K, Popping G, Rix HW, Sargent M, van der Wel A, van der Werf P (2016a) The ALMA Spectroscopic Survey in the Hubble Ultra Deep Field: Molecular Gas Reservoirs in High-redshift Galaxies. *ApJ*833:70, DOI 10.3847/1538-4357/833/1/70, 1607.06771
- Decarli R, Walter F, Aravena M, Carilli C, Bouwens R, da Cunha E, Daddi E, Ivison RJ, Popping G, Riechers D, Smail IR, Swinbank M, Weiss A, Anguita T, Assef RJ, Bauer FE, Bell EF, Bertoldi F, Chapman S, Colina L, Cortes PC, Cox P, Dickinson M, Elbaz D, González-López J, Ibar E, Infante L, Hodge J, Karim A, Le Fevre O, Magnelli B, Neri R, Oesch P, Ota K, Rix HW, Sargent M, Sheth K, van der Wel A, van der Werf P, Wagg J (2016b) ALMA Spectroscopic Survey in the Hubble Ultra Deep Field: CO Luminosity Functions and the Evolution of the Cosmic Density of Molecular Gas. *ApJ*833:69, DOI 10.3847/1538-4357/833/1/69, 1607.06770
- Dekel A, Birnboim Y, Engel G, Freundlich J, Goerdt T, Mumcuoglu M, Neistein E, Pichon C, Teyssier R, Zinger E (2009) Cold streams in early massive hot haloes as the main mode of galaxy formation. *Nature*457:451–454, DOI 10.1038/nature07648, 0808.0553
- Dekel A, Zolotov A, Tweed D, Cacciato M, Ceverino D, Primack JR (2013) Toy models for galaxy formation versus simulations. *MNRAS*435:999–1019, DOI 10.1093/mnras/stt1338, 1303.3009
- Denicoló G, Terlevich R, Terlevich E (2002) New light on the search for low-metallicity galaxies - I. The N2 calibrator. *MNRAS*330:69–74, DOI 10.1046/j.1365-8711.2002.05041.x, astro-ph/0110356
- Dessauges-Zavadsky M, Zamojski M, Schaerer D, Combes F, Egami E, Swinbank AM, Richard J, Sklias P, Rawle TD, Rex M, Kneib JP, Boone F, Blain A (2015) Molecular gas content in strongly lensed  $z \sim 1.5$ -3 star-forming galaxies with low infrared luminosities. *A&A*577:A50, DOI 10.1051/0004-6361/201424661, 1408.0816
- Díaz-Santos T, Armus L, Charmandaris V, Stierwalt S, Murphy EJ, Haan S, Inami H, Malhotra S, Meijerink R, Stacey G, Petric AO, Evans AS, Veilleux S, van der Werf PP, Lord S, Lu N, Howell JH, Appleton P, Mazzarella JM, Surace JA, Xu CK, Schulz B, Sanders DB, Bridge C, Chan BHP, Frayer DT, Iwasawa K, Melbourne J, Sturm E (2013) Explaining the [C II]157.7  $\mu$ m Deficit in Luminous Infrared Galaxies – First Results from a Herschel/PACS Study of the GOALS Sample. *ApJ*774:68, DOI 10.1088/0004-637X/774/1/68, 1307.2635
- Downes D, Solomon PM, Radford SJE (1995) New Observations and a New Interpretation of CO(3–2) in IRAS F10214+4724. *ApJ*453:L65, DOI 10.1086/309754, astro-ph/9508130
- Dunlop JS, McLure RJ, Biggs AD, Geach JE, Michałowski MJ, Ivison RJ, Rujopakarn W, van Kampen E, Kirkpatrick A, Pope A, Scott D, Swinbank AM, Targett TA, Aretxaga I, Austermann JE, Best PN, Bruce VA, Chapin EL, Charlot S, Cirasuolo M, Coppin K, Ellis RS, Finkelstein SL, Hayward CC,

- Hughes DH, Ibar E, Jagannathan P, Khochfar S, Koprowski MP, Narayanan D, Nyland K, Papovich C, Peacock JA, Rieke GH, Robertson B, Vernstrom T, Werf PPvd, Wilson GW, Yun M (2017) A deep ALMA image of the Hubble Ultra Deep Field. *MNRAS*466:861–883, DOI 10.1093/mnras/stw3088, 1606.00227
- Eales S, Dunne L, Clements D, Cooray A, De Zotti G, Dye S, Ivison R, Jarvis M, Lagache G, Maddox S, Negrello M, Serjeant S, Thompson MA, Van Kampen E, Amblard A, Andreani P, Baes M, Beelen A, Bendo GJ, Benford D, Bertoldi F, Bock J, Bonfield D, Boselli A, Bridge C, Buat V, Burgarella D, Carlberg R, Cava A, Chanical P, Charlot S, Christopher N, Coles P, Cortese L, Dariush A, da Cunha E, Dalton G, Danese L, Dannerbauer H, Driver S, Dunlop J, Fan L, Farrah D, Frayer D, Frenk C, Geach J, Gardner J, Gomez H, González-Nuevo J, González-Solares E, Griffin M, Hardcastle M, Hatziminaoglou E, Herranz D, Hughes D, Ibar E, Jeong WS, Lacey C, Lapi A, Lawrence A, Lee M, Leeuw L, Liske J, López-Caniego M, Müller T, Nandra K, Panuzzo P, Papageorgiou A, Patanchon G, Peacock J, Pearson C, Phillipps S, Pohlen M, Popescu C, Rawlings S, Rigby E, Rigopoulou M, Rotherham A, Rodighiero G, Sansom A, Schulz B, Scott D, Smith DJB, Sibthorpe B, Smail I, Stevens J, Sutherland W, Takeuchi T, Tedds J, Temi P, Tuffs R, Trichas M, Vaccari M, Valtchanov I, van der Werf P, Verma A, Viera J, Vlahakis C, White GJ (2010) The Herschel ATLAS. *PASP*122:499, DOI 10.1086/653086, 0910.4279
- Egami E, Rex M, Rawle TD, Pérez-González PG, Richard J, Kneib JP, Schaerer D, Altieri B, Valtchanov I, Blain AW, Fadda D, Zemcov M, Bock JJ, Boone F, Bridge CR, Clement B, Combes F, Dessauges-Zavadsky M, Dowell CD, Ilbert O, Ivison RJ, Jauzac M, Lutz D, Metcalfe L, Omont A, Pelló R, Pereira MJ, Rieke GH, Rodighiero G, Smail I, Smith GP, Tramoy G, Walth GL, van der Werf P, Werner MW (2010) The Herschel Lensing Survey (HLS): Overview. *A&A*518:L12, DOI 10.1051/0004-6361/201014696, 1005.3820
- Elbaz D, Dickinson M, Hwang HS, Díaz-Santos T, Magdis G, Magnelli B, Le Borgne D, Galliano F, Pannella M, Chanical P, Armus L, Charmandaris V, Daddi E, Aussel H, Popesso P, Kartaltepe J, Altieri B, Valtchanov I, Coia D, Dannerbauer H, Dasyra K, Leiton R, Mazzarella J, Alexander DM, Buat V, Burgarella D, Chary RR, Gilli R, Ivison RJ, Juneau S, Le Floc'h E, Lutz D, Morrison GE, Mullaney JR, Murphy E, Pope A, Scott D, Brodwin M, Calzetti D, Cesarsky C, Charlot S, Dole H, Eisenhardt P, Ferguson HC, Förster Schreiber N, Frayer D, Giavalisco M, Huynh M, Koekoer AM, Papovich C, Reddy N, Surace C, Teplitz H, Yun MS, Wilson G (2011) GOODS-Herschel: an infrared main sequence for star-forming galaxies. *A&A*533:A119, DOI 10.1051/0004-6361/201117239, 1105.2537
- Emons BHC, Lehnert MD, Villar-Martín M, Norris RP, Ekers RD, van Moorsel GA, Dannerbauer H, Pentericci L, Miley GK, Allison JR, Sadler EM, Guillard P, Carilli CL, Mao MY, Röttgering HJA, De Breuck C, Seymour N, Gullberg B, Ceverino D, Jagannathan P, Vernet J, Indermuehle BT (2016) Molecular gas in the halo fuels the growth of a massive clus-

- ter galaxy at high redshift. *Science* 354:1128–1130, DOI 10.1126/science.aag0512, 1612.00387
- Emonts BHC, Lehnert MD, Dannerbauer H, De Breuck C, Villar-Martín M, Miley GK, Allison JR, Gullberg B, Hatch NA, Guillard P, Mao MY, Norris RP (2018) Giant galaxy growing from recycled gas: ALMA maps the circumgalactic molecular medium of the Spiderweb in [C I]. *MNRAS*477:L60–L65, DOI 10.1093/mnrasl/sly034, 1802.08742
- Freundlich J, Combes F, Tacconi LJ, Cooper MC, Genzel R, Neri R, Bolatto A, Bournaud F, Burkert A, Cox P, Davis M, Förster Schreiber NM, Garcia-Burillo S, Gracia-Carpio J, Lutz D, Naab T, Newman S, Sternberg A, Weiner B (2013) Towards a resolved Kennicutt-Schmidt law at high redshift. *A&A*553:A130, DOI 10.1051/0004-6361/201220981, 1301.0628
- Genzel R, Tacconi LJ, Combes F, Bolatto A, Neri R, Sternberg A, Cooper MC, Bouché N, Bournaud F, Burkert A, Comerford J, Cox P, Davis M, Förster Schreiber NM, Garcia-Burillo S, Gracia-Carpio J, Lutz D, Naab T, Newman S, Saintonge A, Shapiro K, Shapley A, Weiner B (2012) The Metallicity Dependence of the CO to H<sub>2</sub> Conversion Factor in  $z \geq 1$  Star-forming Galaxies. *ApJ*746:69, DOI 10.1088/0004-637X/746/1/69, 1106.2098
- Genzel R, Tacconi LJ, Lutz D, Saintonge A, Berta S, Magnelli B, Combes F, García-Burillo S, Neri R, Bolatto A, Contini T, Lilly S, Boissier J, Boone F, Bouché N, Bournaud F, Burkert A, Carollo M, Colina L, Cooper MC, Cox P, Feruglio C, Förster Schreiber NM, Freundlich J, Gracia-Carpio J, Juneau S, Kovac K, Lippa M, Naab T, Salome P, Renzini A, Sternberg A, Walter F, Weiner B, Weiss A, Wuyts S (2015) Combined CO and Dust Scaling Relations of Depletion Time and Molecular Gas Fractions with Cosmic Time, Specific Star-formation Rate, and Stellar Mass. *ApJ*800:20, DOI 10.1088/0004-637X/800/1/20, 1409.1171
- Ginolfi M, Maiolino R, Nagao T, Carniani S, Belfiore F, Cresci G, Hatsukade B, Mannucci F, Marconi A, Pallottini A, Schneider R, Santini P (2017) Molecular gas on large circumgalactic scales at  $z = 3.47$ . *MNRAS*468:3468–3483, DOI 10.1093/mnras/stx712, 1611.07026
- Gullberg B, De Breuck C, Vieira JD, Weiß A, Aguirre JE, Aravena M, Béthermin M, Bradford CM, Bothwell MS, Carlstrom JE, Chapman SC, Fassnacht CD, Gonzalez AH, Greve TR, Hezaveh Y, Holzappel WL, Husband K, Ma J, Malkan M, Marrone DP, Menten K, Murphy EJ, Reichardt CL, Spilker JS, Stark AA, Strandet M, Welikala N (2015) The nature of the [C II] emission in dusty star-forming galaxies from the SPT survey. *MNRAS*449:2883–2900, DOI 10.1093/mnras/stv372, 1501.06909
- Hashimoto T, Laporte N, Mawatari K, Ellis RS, Inoue AK, Zackrisson E, Roberts-Borsani G, Zheng W, Tamura Y, Bauer FE, Fletcher T, Harikane Y, Hatsukade B, Hayatsu NH, Matsuda Y, Matsuo H, Okamoto T, Ouchi M, Pello R, Rydberg CE, Shimizu I, Taniguchi Y, Umehata H, Yoshida N (2018) The onset of star formation 250 million years after the Big Bang. *ArXiv e-prints* 1805.05966
- Hatsukade B, Kohno K, Umehata H, Aretxaga I, Caputi KI, Dunlop JS, Ikarashi S, Iono D, Ivison RJ, Lee M, Makiya R, Matsuda Y, Motohara

- K, Nakanishi K, Ohta K, Tadaki Ki, Tamura Y, Wang WH, Wilson GW, Yamaguchi Y, Yun MS (2016) SXDF-ALMA 2-arcmin<sup>2</sup> deep survey: 1.1-mm number counts. *PASJ*68:36, DOI 10.1093/pasj/psw026, 1602.08167
- Ilbert O, McCracken HJ, Le Fèvre O, Capak P, Dunlop J, Karim A, Renzini MA, Caputi K, Boissier S, Arnouts S, Aussel H, Comparat J, Guo Q, Hudelot P, Kartaltepe J, Kneib JP, Krogager JK, Le Floch E, Lilly S, Mellier Y, Milvang-Jensen B, Moutard T, Onodera M, Richard J, Salvato M, Sanders DB, Scoville N, Silverman JD, Taniguchi Y, Tasca L, Thomas R, Toft S, Tresse L, Vergani D, Wolk M, Zirm A (2013) Mass assembly in quiescent and star-forming galaxies since  $z \sim 4$  from UltraVISTA. *A&A*556:A55, DOI 10.1051/0004-6361/201321100, 1301.3157
- Illingworth GD, Magee D, Oesch PA, Bouwens RJ, Labbé I, Stiavelli M, van Dokkum PG, Franx M, Trenti M, Carollo CM, Gonzalez V (2013) The HST eXtreme Deep Field (XDF): Combining All ACS and WFC3/IR Data on the HUDF Region into the Deepest Field Ever. *ApJS*209:6, DOI 10.1088/0067-0049/209/1/6, 1305.1931
- Katz H, Kimm T, Sijacki D, Haehnelt MG (2017) Interpreting ALMA observations of the ISM during the epoch of reionization. *MNRAS*468:4831–4861, DOI 10.1093/mnras/stx608, 1612.01786
- Keating GK, Marrone DP, Bower GC, Leitch E, Carlstrom JE, DeBoer DR (2016) COPSS II: The Molecular Gas Content of Ten Million Cubic Megaparsecs at Redshift  $z \sim 3$ . *ApJ*830:34, DOI 10.3847/0004-637X/830/1/34, 1605.03971
- Keres D, Yun MS, Young JS (2003) CO Luminosity Functions for Far-Infrared- and B-Band-selected Galaxies and the First Estimate for  $\Omega_{HI+H_2}$ . *ApJ*582:659–667, DOI 10.1086/344820, astro-ph/0209413
- Kormendy J, Ho LC (2013) Coevolution (Or Not) of Supermassive Black Holes and Host Galaxies. *ARA&A*51:511–653, DOI 10.1146/annurev-astro-082708-101811, 1304.7762
- Lagos CdP, Bayet E, Baugh CM, Lacey CG, Bell TA, Fanidakis N, Geach JE (2012) Predictions for the CO emission of galaxies from a coupled simulation of galaxy formation and photon-dominated regions. *MNRAS*426:2142–2165, DOI 10.1111/j.1365-2966.2012.21905.x, 1204.0795
- Laporte N, Ellis RS, Boone F, Bauer FE, Quénard D, Roberts-Borsani GW, Pelló R, Pérez-Fournon I, Streblyanska A (2017) Dust in the Reionization Era: ALMA Observations of a  $z = 8.38$  Gravitationally Lensed Galaxy. *ApJ*837:L21, DOI 10.3847/2041-8213/aa62aa, 1703.02039
- Le Fèvre O, Vettolani G, Paltani S, Tresse L, Zamorani G, Le Brun V, Moreau C, Bottini D, Maccagni D, Picat JP, Scaramella R, Scodreggio M, Zanichelli A, Adami C, Arnouts S, Bardelli S, Bolzonella M, Cappi A, Charlot S, Contini T, Foucaud S, Franzetti P, Garilli B, Gavignaud I, Guzzo L, Ilbert O, Iovino A, McCracken HJ, Mancini D, Marano B, Marinoni C, Mathez G, Mazure A, Meneux B, Merighi R, Pelló R, Pollo A, Pozzetti L, Radovich M, Zucca E, Arnaboldi M, Bondi M, Bongiorno A, Busarello G, Ciliegi P, Gregorini L, Mellier Y, Merluzzi P, Ripepi V, Rizzo D (2004) The VIMOS VLT Deep Survey. Public release of 1599 redshifts to  $I_{AB} < 24$  across the

- Chandra Deep Field South. *A&A*428:1043–1049, DOI 10.1051/0004-6361:20048072, [astro-ph/0403628](#)
- Le Floc'h E, Papovich C, Dole H, Bell EF, Lagache G, Rieke GH, Egami E, Pérez-González PG, Alonso-Herrero A, Rieke MJ, Blaylock M, Engelbracht CW, Gordon KD, Hines DC, Misselt KA, Morrison JE, Mould J (2005) Infrared Luminosity Functions from the Chandra Deep Field-South: The Spitzer View on the History of Dusty Star Formation at  $0 < z < 1$ . *ApJ*632:169–190, DOI 10.1086/432789, [astro-ph/0506462](#)
- Lehmer BD, Alexander DM, Geach JE, Smail I, Basu-Zych A, Bauer FE, Chapman SC, Matsuda Y, Scharf CA, Volonteri M, Yamada T (2009) The Chandra Deep Protocluster Survey: Evidence for an Enhancement of AGN Activity in the SSA22 Protocluster at  $z = 3.09$ . *ApJ*691:687–695, DOI 10.1088/0004-637X/691/1/687, 0809.5058
- Leroy AK, Bolatto A, Gordon K, Sandstrom K, Gratier P, Rosolowsky E, Engelbracht CW, Mizuno N, Corbelli E, Fukui Y, Kawamura A (2011) The CO-to-H<sub>2</sub> Conversion Factor from Infrared Dust Emission across the Local Group. *ApJ*737:12, DOI 10.1088/0004-637X/737/1/12, 1102.4618
- Levshakov SA, Combes F, Boone F, Agafonova II, Reimers D, Kozlov MG (2012) An upper limit to the variation in the fundamental constants at redshift  $z = 5.2$ . *A&A*540:L9, DOI 10.1051/0004-6361/201219042, 1203.3649
- Lilly SJ, Carollo CM, Pipino A, Renzini A, Peng Y (2013) Gas Regulation of Galaxies: The Evolution of the Cosmic Specific Star Formation Rate, the Metallicity-Mass-Star-formation Rate Relation, and the Stellar Content of Halos. *ApJ*772:119, DOI 10.1088/0004-637X/772/2/119, 1303.5059
- Luhman KL (2013) Discovery of a Binary Brown Dwarf at 2 pc from the Sun. *ApJ*767:L1, DOI 10.1088/2041-8205/767/1/L1, 1303.2401
- Madau P, Dickinson M (2014) Cosmic Star-Formation History. *ARA&A*52:415–486, DOI 10.1146/annurev-astro-081811-125615, 1403.0007
- Maiolino R, Cox P, Caselli P, Beelen A, Bertoldi F, Carilli CL, Kaufman MJ, Menten KM, Nagao T, Omont A, Weiß A, Walmsley CM, Walter F (2005) First detection of [CII]158  $\mu\text{m}$  at high redshift: vigorous star formation in the early universe. *A&A*440:L51–L54, DOI 10.1051/0004-6361:200500165, [astro-ph/0508064](#)
- Maiolino R, Nagao T, Grazian A, Cocchia F, Marconi A, Mannucci F, Cimatti A, Pipino A, Ballero S, Calura F, Chiappini C, Fontana A, Granato GL, Matteucci F, Pastorini G, Pentericci L, Risaliti G, Salvati M, Silva L (2008) AMAZE. I. The evolution of the mass-metallicity relation at  $z > 3$ . *A&A*488:463–479, DOI 10.1051/0004-6361:200809678, 0806.2410
- Maiolino R, Carniani S, Fontana A, Vallini L, Pentericci L, Ferrara A, Vanzella E, Grazian A, Gallerani S, Castellano M, Cristiani S, Brammer G, Santini P, Wagg J, Williams R (2015) The assembly of ‘normal’ galaxies at  $z \sim 7$  probed by ALMA. *MNRAS*452:54–68, DOI 10.1093/mnras/stv1194, 1502.06634
- Malhotra S, Kaufman MJ, Hollenbach D, Helou G, Rubin RH, Brauher J,

- Dale D, Lu NY, Lord S, Stacey G, Contursi A, Hunter DA, Dinerstein H (2001) Far-Infrared Spectroscopy of Normal Galaxies: Physical Conditions in the Interstellar Medium. *ApJ*561:766–786, DOI 10.1086/323046, [astro-ph/0106485](#)
- Malhotra S, Rhoads JE, Finkelstein K, Yang H, Carilli C, Combes F, Dassis K, Finkelstein S, Frye B, Gerin M, Guillard P, Nesvadba N, Rigby J, Shin MS, Spaans M, Strauss MA, Papovich C (2017) Herschel Extreme Lensing Line Observations: [CII] Variations in Galaxies at Redshifts  $z=1-3$ . *ApJ*835:110, DOI 10.3847/1538-4357/835/1/110
- Matsuda Y, Yamada T, Hayashino T, Tamura H, Yamauchi R, Ajiki M, Fujita SS, Murayama T, Nagao T, Ohta K, Okamura S, Ouchi M, Shimasaku K, Shioya Y, Taniguchi Y (2004) A Subaru Search for Ly $\alpha$  Blobs in and around the Protocluster Region At Redshift  $z = 3.1$ . *AJ*128:569–584, DOI 10.1086/422020, [astro-ph/0405221](#)
- Matthee J, Sobral D, Boone F, Röttgering H, Schaerer D, Girard M, Pallottini A, Vallini L, Ferrara A, Darvish B, Mobasher B (2017) ALMA Reveals Metals yet No Dust within Multiple Components in CR7. *ApJ*851:145, DOI 10.3847/1538-4357/aa9931, 1709.06569
- Muller S, Combes F, Guélin M, Gérin M, Aalto S, Beelen A, Black JH, Curran SJ, Darling J, V-Trung D, García-Burillo S, Henkel C, Horellou C, Martín S, Martí-Vidal I, Menten KM, Murphy MT, Ott J, Wiklind T, Zwaan MA (2014) An ALMA Early Science survey of molecular absorption lines toward PKS 1830-211. Analysis of the absorption profiles. *A&A*566:A112, DOI 10.1051/0004-6361/201423646, 1404.7667
- Muller S, Müller HSP, Black JH, Beelen A, Combes F, Curran S, Gérin M, Guélin M, Henkel C, Martín S, Aalto S, Falgarone E, Menten KM, Schilke P, Wiklind T, Zwaan MA (2016) OH<sup>+</sup> and H<sub>2</sub>O<sup>+</sup> absorption toward PKS 1830-211. *A&A*595:A128, DOI 10.1051/0004-6361/201629073, 1609.01060
- Negrello M, Hopwood R, De Zotti G, Cooray A, Verma A, Bock J, Frayer DT, Gurwell MA, Omont A, Neri R, Dannerbauer H, Leeuw LL, Barton E, Cooke J, Kim S, da Cunha E, Rodighiero G, Cox P, Bonfield DG, Jarvis MJ, Serjeant S, Ivison RJ, Dye S, Aretxaga I, Hughes DH, Ibar E, Bertoldi F, Valtchanov I, Eales S, Dunne L, Driver SP, Auld R, Buttiglione S, Cava A, Grady CA, Clements DL, Dariush A, Fritz J, Hill D, Hornbeck JB, Kelvin L, Lagache G, Lopez-Caniego M, Gonzalez-Nuevo J, Maddox S, Pascale E, Pohlen M, Rigby EE, Robotham A, Simpson C, Smith DJB, Temi P, Thompson MA, Woodgate BE, York DG, Aguirre JE, Beelen A, Blain A, Baker AJ, Birkinshaw M, Blundell R, Bradford CM, Burgarella D, Danese L, Dunlop JS, Fleuren S, Glenn J, Harris AI, Kamenetzky J, Lupu RE, Maddalena RJ, Madore BF, Maloney PR, Matsuhara H, Michałowski MJ, Murphy EJ, Naylor BJ, Nguyen H, Popescu C, Rawlings S, Rigopoulou D, Scott D, Scott KS, Seibert M, Smail I, Tuffs RJ, Vieira JD, van der Werf PP, Zmuidzinas J (2010) The Detection of a Population of Submillimeter-Bright, Strongly Lensed Galaxies. *Science* 330:800, DOI 10.1126/science.1193420, 1011.1255
- Obreschkow D, Croton D, De Lucia G, Khochfar S, Rawlings S (2009) Simula-

- tion of the Cosmic Evolution of Atomic and Molecular Hydrogen in Galaxies. *ApJ*698:1467–1484, DOI 10.1088/0004-637X/698/2/1467, 0904.2221
- Omont A (2007) Molecules in galaxies. *Reports on Progress in Physics* 70:1099–1176, DOI 10.1088/0034-4885/70/7/R03, 0709.3814
- Oteo I, Zhang ZY, Yang C, Ivison RJ, Omont A, Bremer M, Bussmann S, Cooray A, Cox P, Dannerbauer H, Dunne L, Eales S, Furlanetto C, Gavazzi R, Gao Y, Greve TR, Nayyeri H, Negrello M, Neri R, Riechers D, Tunnard R, Wagg J, Van der Werf P (2017) High Dense Gas Fraction in Intensely Star-forming Dusty Galaxies. *ApJ*850:170, DOI 10.3847/1538-4357/aa8ee3, 1701.05901
- Ouchi M, Ellis R, Ono Y, Nakanishi K, Kohno K, Momose R, Kurono Y, Ashby MLN, Shimasaku K, Willner SP, Fazio GG, Tamura Y, Iono D (2013) An Intensely Star-forming Galaxy at  $z \sim 7$  with Low Dust and Metal Content Revealed by Deep ALMA and HST Observations. *ApJ*778:102, DOI 10.1088/0004-637X/778/2/102, 1306.3572
- Pan Z, Zheng X, Lin W, Li J, Wang J, Fan L, Kong X (2016) The Spatially Resolved NUV- $r$  Color of Local Star-forming Galaxies and Clues for Quenching. *ApJ*819:91, DOI 10.3847/0004-637X/819/2/91, 1601.05503
- Papadopoulos PP, van der Werf P, Isaak K, Xilouris EM (2010) CO Spectral Line Energy Distributions of Infrared-Luminous Galaxies and Active Galactic Nuclei. *ApJ*715:775–792, DOI 10.1088/0004-637X/715/2/775, 1003.5889
- Peng Yj, Lilly SJ, Kovač K, Bolzonella M, Pozzetti L, Renzini A, Zamorani G, Ilbert O, Knobel C, Iovino A, Maier C, Cucciati O, Tasca L, Carollo CM, Silverman J, Kampeczyk P, de Ravel L, Sanders D, Scoville N, Contini T, Mainieri V, Scodreggio M, Kneib JP, Le Fèvre O, Bardelli S, Bongiorno A, Caputi K, Coppia G, de la Torre S, Franzetti P, Garilli B, Lamareille F, Le Borgne JF, Le Brun V, Mignoli M, Perez Montero E, Pello R, Ricciardelli E, Tanaka M, Tresse L, Vergani D, Welikala N, Zucca E, Oesch P, Abbas U, Barnes L, Bordoloi R, Bottini D, Cappi A, Cassata P, Cimatti A, Fumana M, Hasinger G, Koekemoer A, Leauthaud A, Maccagni D, Marinoni C, McCracken H, Memeo P, Meneux B, Nair P, Porciani C, Presotto V, Scaramella R (2010) Mass and Environment as Drivers of Galaxy Evolution in SDSS and zCOSMOS and the Origin of the Schechter Function. *ApJ*721:193–221, DOI 10.1088/0004-637X/721/1/193, 1003.4747
- Pentericci L, Carniani S, Castellano M, Fontana A, Maiolino R, Guaita L, Vanzella E, Grazian A, Santini P, Yan H, Cristiani S, Conselice C, Giavalisco M, Hathi N, Koekemoer A (2016) Tracing the Reionization Epoch with ALMA: [C II] Emission in  $z \sim 7$  Galaxies. *ApJ*829:L11, DOI 10.3847/2041-8205/829/1/L11, 1608.08837
- Popping G, Somerville RS, Trager SC (2014) Evolution of the atomic and molecular gas content of galaxies. *MNRAS*442:2398–2418, DOI 10.1093/mnras/stu991, 1308.6764
- Prochaska JX, Herbert-Fort S, Wolfe AM (2005) The SDSS Damped Ly $\alpha$  Survey: Data Release 3. *ApJ*635:123–142, DOI 10.1086/497287, astro-ph/0508361

- Rafelski M, Teplitz HI, Gardner JP, Coe D, Bond NA, Koekemoer AM, Grogin N, Kurczynski P, McGrath EJ, Bourque M, Atek H, Brown TM, Colbert JW, Codoreanu A, Ferguson HC, Finkelstein SL, Gawiser E, Giavalisco M, Gronwall C, Hanish DJ, Lee KS, Mehta V, de Mello DF, Ravindranath S, Ryan RE, Scarlata C, Siana B, Soto E, Voyer EN (2015) UVUDF: Ultraviolet Through Near-infrared Catalog and Photometric Redshifts of Galaxies in the Hubble Ultra Deep Field. *AJ*150:31, DOI 10.1088/0004-6256/150/1/31, 1505.01160
- Riechers DA, Bradford CM, Clements DL, Dowell CD, Pérez-Fournon I, Ivison RJ, Bridge C, Conley A, Fu H, Vieira JD, Wardlow J, Calanog J, Cooray A, Hurley P, Neri R, Kamenetzky J, Aguirre JE, Altieri B, Arumugam V, Benford DJ, Béthermin M, Bock J, Burgarella D, Cabrera-Lavers A, Chapman SC, Cox P, Dunlop JS, Earle L, Farrah D, Ferrero P, Franceschini A, Gavazzi R, Glenn J, Solares EAG, Gurwell MA, Halpern M, Hatziminaoglou E, Hyde A, Ibar E, Kovács A, Krips M, Lupu RE, Maloney PR, Martinez-Navajas P, Matsuhara H, Murphy EJ, Naylor BJ, Nguyen HT, Oliver SJ, Omont A, Page MJ, Petitpas G, Rangwala N, Roseboom IG, Scott D, Smith AJ, Staguhn JG, Streblyanska A, Thomson AP, Valtchanov I, Viero M, Wang L, Zemcov M, Zmuidzinas J (2013) A dust-obscured massive maximum-starburst galaxy at a redshift of 6.34. *Nature*496:329–333, DOI 10.1038/nature12050, 1304.4256
- Riechers DA, Carilli CL, Capak PL, Scoville NZ, Smolčić V, Schinnerer E, Yun M, Cox P, Bertoldi F, Karim A, Yan L (2014) ALMA Imaging of Gas and Dust in a Galaxy Protocluster at Redshift 5.3: [C II] Emission in “Typical” Galaxies and Dusty Starbursts  $\sim 1$  Billion Years after the Big Bang. *ApJ*796:84, DOI 10.1088/0004-637X/796/2/84, 1404.7159
- Salim DM, Federrath C, Kewley LJ (2015) A Universal, Turbulence-regulated Star Formation Law: From Milky Way Clouds to High-redshift Disk and Starburst Galaxies. *ApJ*806:L36, DOI 10.1088/2041-8205/806/2/L36, 1505.03144
- Sanders DB, Mirabel IF (1996) Luminous Infrared Galaxies. *ARA&A*34:749, DOI 10.1146/annurev.astro.34.1.749
- Sargent MT, Daddi E, Béthermin M, Aussel H, Magdis G, Hwang HS, Juneau S, Elbaz D, da Cunha E (2014) Regularity Underlying Complexity: A Redshift-independent Description of the Continuous Variation of Galaxy-scale Molecular Gas Properties in the Mass-star Formation Rate Plane. *ApJ*793:19, DOI 10.1088/0004-637X/793/1/19, 1303.4392
- Schaerer D, Boone F, Zamojski M, Staguhn J, Dessauges-Zavadsky M, Finkelstein S, Combes F (2015) New constraints on dust emission and UV attenuation of  $z = 6.5$ - $7.5$  galaxies from millimeter observations. *A&A*574:A19, DOI 10.1051/0004-6361/201424649, 1407.5793
- Schinnerer E, Groves B, Sargent MT, Karim A, Oesch PA, Magnelli B, LeFevre O, Tasca L, Civano F, Cassata P, Smolčić V (2016) Gas Fraction and Depletion Time of Massive Star-forming Galaxies at  $z \sim 3.2$ : No Change in Global Star Formation Process out to  $z > 3$ . *ApJ*833:112, DOI 10.3847/1538-4357/833/1/112, 1610.03656

- Scoville N, Aussel H, Sheth K, Scott KS, Sanders D, Ivison R, Pope A, Capak P, Vanden Bout P, Manohar S, Kartaltepe J, Robertson B, Lilly S (2014) The Evolution of Interstellar Medium Mass Probed by Dust Emission: ALMA Observations at  $z = 0.3-2$ . *ApJ*783:84, DOI 10.1088/0004-637X/783/2/84, 1401.2987
- Scoville N, Sheth K, Aussel H, Vanden Bout P, Capak P, Bongiorno A, Casey CM, Murchikova L, Koda J, Álvarez-Márquez J, Lee N, Laigle C, McCracken HJ, Ilbert O, Pope A, Sanders D, Chu J, Toft S, Ivison RJ, Manohar S (2016) ISM Masses and the Star formation Law at  $Z = 1$  to 6: ALMA Observations of Dust Continuum in 145 Galaxies in the COSMOS Survey Field. *ApJ*820:83, DOI 10.3847/0004-637X/820/2/83, 1511.05149
- Scoville N, Lee N, Vanden Bout P, Diaz-Santos T, Sanders D, Darvish B, Bongiorno A, Casey CM, Murchikova L, Koda J, Capak P, Vlahakis C, Ilbert O, Sheth K, Morokuma-Matsui K, Ivison RJ, Aussel H, Laigle C, McCracken HJ, Armus L, Pope A, Toft S, Masters D (2017) Evolution of Interstellar Medium, Star Formation, and Accretion at High Redshift. *ApJ*837:150, DOI 10.3847/1538-4357/aa61a0, 1702.04729
- Sharda P, Federrath C, da Cunha E, Swinbank AM, Dye S (2018) Testing star formation laws in a starburst galaxy at redshift 3 resolved with ALMA. *MNRAS*477:4380–4390, DOI 10.1093/mnras/sty886, 1712.03661
- Solomon PM, Vanden Bout PA (2005) Molecular Gas at High Redshift. *ARA&A*43:677–725, DOI 10.1146/annurev.astro.43.051804.102221, astro-ph/0508481
- Speagle JS, Steinhardt CL, Capak PL, Silverman JD (2014) A Highly Consistent Framework for the Evolution of the Star-Forming “Main Sequence” from  $z \sim 0-6$ . *ApJS*214:15, DOI 10.1088/0067-0049/214/2/15, 1405.2041
- Spilker J, Bezanson R, Barisic I, Bell E, Lagos CdP, Maseda M, Muzzin A, Pacifici C, Sobral D, Straatman C, van der Wel A, van Dokkum P, Weiner B, Whitaker K, Williams CC, Wu PF (2018) Molecular Gas Contents and Scaling Relations for Massive Passive Galaxies at Intermediate Redshifts from the LEGA-C Survey. *ArXiv e-prints* 1805.02667
- Stark DP (2016) Galaxies in the First Billion Years After the Big Bang. *ARA&A*54:761–803, DOI 10.1146/annurev-astro-081915-023417
- Steidel CC, Adelberger KL, Shapley AE, Pettini M, Dickinson M, Giavalisco M (2000)  $Ly\alpha$  Imaging of a Proto-Cluster Region at  $z=3.09$ . *ApJ*532:170–182, DOI 10.1086/308568, astro-ph/9910144
- Strandet ML, Weiss A, Vieira JD, de Breuck C, Aguirre JE, Aravena M, Ashby MLN, Béthermin M, Bradford CM, Carlstrom JE, Chapman SC, Crawford TM, Everett W, Fassnacht CD, Furstenau RM, Gonzalez AH, Greve TR, Gullberg B, Hezaveh Y, Kamenetzky JR, Litke K, Ma J, Malkan M, Marrone DP, Menten KM, Murphy EJ, Nadolski A, Rotermund KM, Spilker JS, Stark AA, Welikala N (2016) The Redshift Distribution of Dusty Star-forming Galaxies from the SPT Survey. *ApJ*822:80, DOI 10.3847/0004-637X/822/2/80, 1603.05094
- Suess KA, Bezanson R, Spilker JS, Kriek M, Greene JE, Feldmann R, Hunt Q, Narayanan D (2017) Massive Quenched Galaxies at  $z \sim 0.7$  Retain Large

- Molecular Gas Reservoirs. *ApJ*846:L14, DOI 10.3847/2041-8213/aa85dc, 1708.03337
- Swinbank AM, Simpson JM, Smail I, Harrison CM, Hodge JA, Karim A, Walter F, Alexander DM, Brandt WN, de Breuck C, da Cunha E, Chapman SC, Coppin KEK, Danielson ALR, Dannerbauer H, Decarli R, Greve TR, Ivison RJ, Knudsen KK, Lagos CDP, Schinnerer E, Thomson AP, Wardlow JL, Weiß A, van der Werf P (2014) An ALMA survey of sub-millimetre Galaxies in the Extended Chandra Deep Field South: the far-infrared properties of SMGs. *MNRAS*438:1267–1287, DOI 10.1093/mnras/stt2273, 1310.6362
- Tacchella S, Dekel A, Carollo CM, Ceverino D, DeGraf C, Lapiner S, Mandelker N, Primack Joel R (2016) The confinement of star-forming galaxies into a main sequence through episodes of gas compaction, depletion and replenishment. *MNRAS*457:2790–2813, DOI 10.1093/mnras/stw131, 1509.02529
- Tacconi LJ, Genzel R, Neri R, Cox P, Cooper MC, Shapiro K, Bolatto A, Bouché N, Bournaud F, Burkert A, Combes F, Comerford J, Davis M, Schreiber NMF, García-Burillo S, Gracia-Carpio J, Lutz D, Naab T, Omont A, Shapley A, Sternberg A, Weiner B (2010) High molecular gas fractions in normal massive star-forming galaxies in the young Universe. *Nature*463:781–784, DOI 10.1038/nature08773, 1002.2149
- Tacconi LJ, Neri R, Genzel R, Combes F, Bolatto A, Cooper MC, Wuyts S, Bournaud F, Burkert A, Comerford J, Cox P, Davis M, Förster Schreiber NM, García-Burillo S, Gracia-Carpio J, Lutz D, Naab T, Newman S, Omont A, Saintonge A, Shapiro Griffin K, Shapley A, Sternberg A, Weiner B (2013) PHIBSS: Molecular Gas Content and Scaling Relations in  $z \sim 1$ -3 Massive, Main-sequence Star-forming Galaxies. *ApJ*768:74, DOI 10.1088/0004-637X/768/1/74, 1211.5743
- Tacconi LJ, Genzel R, Saintonge A, Combes F, García-Burillo S, Neri R, Bolatto A, Contini T, Förster Schreiber NM, Lilly S, Lutz D, Wuyts S, Accurso G, Boissier J, Boone F, Bouché N, Bournaud F, Burkert A, Carollo M, Cooper M, Cox P, Feruglio C, Freundlich J, Herrera-Camus R, Juneau S, Lippa M, Naab T, Renzini A, Salome P, Sternberg A, Tadaki K, Übler H, Walter F, Weiner B, Weiss A (2018) PHIBSS: Unified Scaling Relations of Gas Depletion Time and Molecular Gas Fractions. *ApJ*853:179, DOI 10.3847/1538-4357/aaa4b4, 1702.01140
- Tadaki Ki, Kohno K, Kodama T, Ikarashi S, Aretxaga I, Berta S, Caputi KI, Dunlop JS, Hatsukade B, Hayashi M, Hughes DH, Ivison R, Izumi T, Koyama Y, Lutz D, Makiya R, Matsuda Y, Nakanishi K, Rujopakarn W, Tamura Y, Umehata H, Wang WH, Wilson GW, Wuyts S, Yamaguchi Y, Yun MS (2015) SXDF-ALMA 1.5 arcmin<sup>2</sup> Deep Survey: A Compact Dusty Star-forming Galaxy at  $z = 2.5$ . *ApJ*811:L3, DOI 10.1088/2041-8205/811/1/L3, 1508.05950
- Tamura Y, Mawatari K, Hashimoto T, Inoue AK, Zackrisson E, Christensen L, Binggeli C, Matsuda Y, Matsuo H, Takeuchi TT, Asano RS, Shimizu I, Okamoto T, Yoshida N, Lee M, Shibuya T, Taniguchi Y, Umehata H, Hatsukade B, Kohno K, Ota K (2018) Detection of the Far-infrared [O III]

- and Dust Emission in a Galaxy at Redshift 8.312: Early Metal Enrichment in the Heart of the Reionization Era. ArXiv e-prints 1806.04132
- Tremblay GR, Oonk JBR, Combes F, Salomé P, O’Dea CP, Baum SA, Voit GM, Donahue M, McNamara BR, Davis TA, McDonald MA, Edge AC, Clarke TE, Galván-Madrid R, Bremer MN, Edwards LOV, Fabian AC, Hamer S, Li Y, Maury A, Russell HR, Quillen AC, Urry CM, Sanders JS, Wise MW (2016) Cold, clumpy accretion onto an active supermassive black hole. *Nature*534:218–221, DOI 10.1038/nature17969, 1606.02304
- van der Werf PP, Isaak KG, Meijerink R, Spaans M, Rykala A, Fulton T, Loenen AF, Walter F, Weiß A, Armus L, Fischer J, Israel FP, Harris AI, Veilleux S, Henkel C, Savini G, Lord S, Smith HA, González-Alfonso E, Naylor D, Aalto S, Charmandaris V, Dasyra KM, Evans A, Gao Y, Greve TR, Güsten R, Kramer C, Martín-Pintado J, Mazzarella J, Papadopoulos PP, Sanders DB, Spinoglio L, Stacey G, Vlahakis C, Wiedner MC, Xilouris EM (2010) Black hole accretion and star formation as drivers of gas excitation and chemistry in Markarian 231. *A&A*518:L42, DOI 10.1051/0004-6361/201014682, 1005.2877
- Venemans BP, McMahan RG, Walter F, Decarli R, Cox P, Neri R, Hewett P, Mortlock DJ, Simpson C, Warren SJ (2012) Detection of Atomic Carbon [C II] 158  $\mu\text{m}$  and Dust Emission from a  $z = 7.1$  Quasar Host Galaxy. *ApJ*751:L25, DOI 10.1088/2041-8205/751/2/L25, 1203.5844
- Venemans BP, Walter F, Zschaechner L, Decarli R, De Rosa G, Findlay JR, McMahan RG, Sutherland WJ (2016) Bright [C II] and Dust Emission in Three  $z > 6.6$  Quasar Host Galaxies Observed by ALMA. *ApJ*816:37, DOI 10.3847/0004-637X/816/1/37, 1511.07432
- Venemans BP, Walter F, Decarli R, Ferkinhoff C, Weiß A, Findlay JR, McMahan RG, Sutherland WJ, Meijerink R (2017) Molecular Gas in Three  $z \sim 7$  Quasar Host Galaxies. *ApJ*845:154, DOI 10.3847/1538-4357/aa81cb, 1707.05238
- Vieira JD, Marrone DP, Chapman SC, De Breuck C, Hezaveh YD, Weiß A, Aguirre JE, Aird KA, Aravena M, Ashby MLN, Bayliss M, Benson BA, Biggs AD, Bleem LE, Bock JJ, Bothwell M, Bradford CM, Brodwin M, Carlstrom JE, Chang CL, Crawford TM, Crites AT, de Haan T, Dobbs MA, Fomalont EB, Fassnacht CD, George EM, Gladders MD, Gonzalez AH, Greve TR, Gullberg B, Halverson NW, High FW, Holder GP, Holzappel WL, Hoover S, Hrubes JD, Hunter TR, Keisler R, Lee AT, Leitch EM, Lueker M, Luong-van D, Malkan M, McIntyre V, McMahan JJ, Mehl J, Menten KM, Meyer SS, Mocz LM, Murphy EJ, Natoli T, Padin S, Plagge T, Reichardt CL, Rest A, Ruel J, Ruhl JE, Sharon K, Schaffer KK, Shaw L, Shirokoff E, Spilker JS, Stalder B, Staniszewski Z, Stark AA, Story K, Vanderlinde K, Welikala N, Williamson R (2013) Dusty starburst galaxies in the early Universe as revealed by gravitational lensing. *Nature*495:344–347, DOI 10.1038/nature12001, 1303.2723
- Walter F, Decarli R, Sargent M, Carilli C, Dickinson M, Riechers D, Ellis R, Stark D, Weiner B, Aravena M, Bell E, Bertoldi F, Cox P, Da Cunha E, Daddi E, Downes D, Lentati L, Maiolino R, Menten KM, Neri R, Rix HW,

- Weiss A (2014) A Molecular Line Scan in the Hubble Deep Field North: Constraints on the CO Luminosity Function and the Cosmic H<sub>2</sub> Density. *ApJ*782:79, DOI 10.1088/0004-637X/782/2/79, 1312.6365
- Walter F, Decarli R, Aravena M, Carilli C, Bouwens R, da Cunha E, Daddi E, Ivison RJ, Riechers D, Smail I, Swinbank M, Weiss A, Anguita T, Assef R, Bacon R, Bauer F, Bell EF, Bertoldi F, Chapman S, Colina L, Cortes PC, Cox P, Dickinson M, Elbaz D, González-López J, Ibar E, Inami H, Infante L, Hodge J, Karim A, Le Fevre O, Magnelli B, Neri R, Oesch P, Ota K, Popping G, Rix HW, Sargent M, Sheth K, van der Wel A, van der Werf P, Wagg J (2016) ALMA Spectroscopic Survey in the Hubble Ultra Deep Field: Survey Description. *ApJ*833:67, DOI 10.3847/1538-4357/833/1/67, 1607.06768
- Wang R, Wagg J, Carilli CL, Walter F, Lentati L, Fan X, Riechers DA, Bertoldi F, Narayanan D, Strauss MA, Cox P, Omont A, Menten KM, Knudsen KK, Neri R, Jiang L (2013) Star Formation and Gas Kinematics of Quasar Host Galaxies at  $z \sim 6$ : New Insights from ALMA. *ApJ*773:44, DOI 10.1088/0004-637X/773/1/44, 1302.4154
- Weiß A, Downes D, Neri R, Walter F, Henkel C, Wilner DJ, Wagg J, Wiklind T (2007) Highly-excited CO emission in APM 08279+5255 at  $z = 3.9$ . *A&A*467:955–969, DOI 10.1051/0004-6361:20066117, astro-ph/0702669
- Whitaker KE, van Dokkum PG, Brammer G, Franx M (2012) The Star Formation Mass Sequence Out to  $z = 2.5$ . *ApJ*754:L29, DOI 10.1088/2041-8205/754/2/L29, 1205.0547
- Whitaker KE, Franx M, Leja J, van Dokkum PG, Henry A, Skelton RE, Fumagalli M, Momcheva IG, Brammer GB, Labbé I, Nelson EJ, Rigby JR (2014) Constraining the Low-mass Slope of the Star Formation Sequence at  $0.5 < z < 2.5$ . *ApJ*795:104, DOI 10.1088/0004-637X/795/2/104, 1407.1843
- Wiklind T, Combes F, Kanekar N (2018) ALMA Observations of Molecular Absorption in the Gravitational Lens PMN 0134-0931. ArXiv e-prints 1804.05377
- Willott CJ, Carilli CL, Wagg J, Wang R (2015) Star Formation and the Interstellar Medium in  $z > 6$  UV-luminous Lyman-break Galaxies. *ApJ*807:180, DOI 10.1088/0004-637X/807/2/180, 1504.05875
- Wuyts S, Förster Schreiber NM, van der Wel A, Magnelli B, Guo Y, Genzel R, Lutz D, Aussel H, Barro G, Berta S, Cava A, Graciá-Carpio J, Hathi NP, Huang KH, Kocevski DD, Koekemoer AM, Lee KS, Le Floch E, McGrath EJ, Nordon R, Popesso P, Pozzi F, Riguccini L, Rodighiero G, Saintonge A, Tacconi L (2011) Galaxy Structure and Mode of Star Formation in the SFR-Mass Plane from  $z \sim 2.5$  to  $z \sim 0.1$ . *ApJ*742:96, DOI 10.1088/0004-637X/742/2/96, 1107.0317